DOCTORAL THESIS

学位論文

CRMP2-binding compound, edonerpic maleate accelerates motor function recovery from brain injury

（CRMP2 に結合する低分子化合物 edonerpic maleate の脳損傷後運動機能回復促進作用）

April, 2019

（2019 年, 4 月）

Hiroki Abe

阿部　弘基

Physiology

Yokohama City University Graduate School of Medicine

横浜市立大学　大学院医学研究科　生理学

Doctoral Supervisor：Takuya Takahashi, Professor

指導教員：高橋　琢哉 教授

NEUROSCIENCE

CRMP2-binding compound, edonerpic maleate, accelerates motor function recovery from brain damage

Hiroki Abe,[1]* Susumu Jitsuki,[1]* Waki Nakajima,[1]* Yumi Murata,[2]*
Aoi Jitsuki-Takahashi,[1] Yuki Katsuno,[1] Hirobumi Tada,[1] Akane Sano,[1] Kumiko Suyama,[1]
Nobuyuki Mochizuki,[1,3,4] Takashi Komori,[1,3,4] Hitoshi Masuyama,[1,3,4]
Tomohiro Okuda,[3,4] Yoshio Goshima,[5] Noriyuki Higo,[2] Takuya Takahashi[1]†

Brain damage such as stroke is a devastating neurological condition that may severely compromise patient quality of life. No effective medication-mediated intervention to accelerate rehabilitation has been established. We found that a small compound, edonerpic maleate, facilitated experience-driven synaptic glutamate AMPA (α-amino-3-hydroxy-5-methyl-4-isoxazole-propionic-acid) receptor delivery and resulted in the acceleration of motor function recovery after motor cortex cryoinjury in mice in a training-dependent manner through cortical reorganization. Edonerpic bound to collapsin-response-mediator-protein 2 (CRMP2) and failed to augment recovery in CRMP2-deficient mice. Edonerpic maleate enhanced motor function recovery from internal capsule hemorrhage in nonhuman primates. Thus, edonerpic maleate, a neural plasticity enhancer, could be a clinically potent small compound with which to accelerate rehabilitation after brain damage.

Brain damage mainly caused by stroke is a severe neurological condition that may lead to paralysis and compromise work capacity and self-care. No pharmacological intervention that could foster recovery and complement current rehabilitation has yet been established as effective. Restoration of motor impairment after brain damage is considered to be the result of compensatory neural plasticity in intact brain regions, mediated by the reorganization of cortical motor maps (1–7). Experience-dependent synaptic AMPA (α-amino-3-hydroxy-5-methyl-4-isoxazole-propionic-acid) receptor (AMPAR) delivery underlies behaviors that require neural plasticity such as learning (8–18). We have previously shown that synaptic AMPAR trafficking plays crucial roles in the compensatory cortical reorganization of the sensory cortex (15). Thus, the facilitation of experience-dependent synaptic AMPAR delivery could result in rehabilitative training-dependent motor cortical reorganization and the acceleration of motor function recovery with rehabilitation after brain damage. Collapsin-

response-mediator-protein 2 (CRMP2) is a downstream molecule of semaphorin (19, 20) and is thought to be related to synaptic plasticity and learning (21, 22).

Results

Edonerpic maleate facilitates experience-dependent synaptic AMPAR delivery in the adult mice barrel cortex

Edonerpic maleate (T-817MA; 1-{3-[2-(1-benzothiophen-5-yl)ethoxy]propyl}azetidin-3-ol maleate) (Fig. 1A) protects neuronal cells and modifies their morphology (23). Edonerpic maleate has been the most characterized compound among this series of compounds. Further, phase I of a clinical trial of edonerpic maleate was successfully terminated, and the safety of edonerpic maleate was proven. However, its clinical application has not been determined. In order to explore actions of edonerpic maleate on neuronal function, we focused on the roles of edonerpic maleate in experience-dependent synaptic plasticity, which has not been studied. To examine whether edonerpic maleate affects experience-dependent synaptic AMPAR delivery, we focused on layer 4–2/3 pyramidal synapses of adult mice barrel cortex, where natural whisker experience–dependent AMPAR delivery is not observed (Fig. 1, B and C). We administered edonerpic maleate orally, twice a day (30 mg/kg) for 3 weeks to 2-month-old adult mice. Then, we prepared acute brain slices and examined synaptic responses at layer 4–2/3 pyramidal synapses of the barrel cortex. We first recorded the ratio of evoked AMPAR- to NMDA

(N-methyl-D-aspartate) receptor (NMDAR)–mediated synaptic currents (AMPA/NMDA ratio). We found an increased AMPA/NMDA ratio in edonerpic maleate–administered compared with vehicle-administered mice (Fig. 1B). This effect was whisker experience–dependent because we detected no increase of the AMPA/NMDA ratio in edonerpic maleate–administered mice in the absence of whiskers (deprived for 2 or 3 days) (Fig. 1B). There was no difference in kinetics of NMDAR-mediated currents among these groups (fig. S1). We then replaced extracellular Ca^{2+} with Sr^{2+} in order to induce asynchronous transmitter release and analyzed the quantal EPSCs (excitatory postsynaptic currents) at layer 4–2/3 pyramidal synapses. We found increased amplitude of evoked miniature EPSCs (mEPSCs) in edonerpic maleate–administered mice, compared with vehicle-administered mice, in the presence but not in the absence of whiskers (Fig. 1C). Three days of treatment with edonerpic maleate exhibited the same effect (fig. S2). Consistent with this, the induction of long-term potentiation (LTP) at layer 4–2/3 barrel cortical synapses onto pyramidal neurons was facilitated by the presence of edonerpic maleate (fig. S3).

Edonerpic maleate binds to CRMP2

We prepared affinity columns of edonerpic-conjugated resin (edonerpic beads) (fig. S4A), only linker-conjugated resin (linker beads), or inactivated control resin (control beads). After the protein purification, we analyzed purified proteins and detected a band near 60 kDa specific to purified proteins by edonerpic beads (Fig. 1D). Mass spectrometry revealed that this band corresponded to CRMP2 (Fig. 1E). Immunoblotting of mice brain lysate pulled down by edonerpic beads (but not linker beads or control beads) also detected the CRMP2-specific band (Fig. 1F). To further examine the binding of edonerpic to CRMP2, we pulled down the brain lysate obtained from CRMP2-deficient mice with edonerpic beads (24). We did not observe detectable CRMP2-positive bands with CRMP2-deficient mice (fig. S4B). We performed isothermal titration calorimetry (ITC) with cell-free conditions and found that the dissociation constant (K_d) value of the edonerpic-binding to CRMP2 at ~7.35×10^{-4} M (Fig. 1G). To further investigate the effect of edonerpic on CRMP2, we mixed purified CRMP2 with edonerpic maleate in a cell-free condition and analyzed with native poly-acrylamide gel electrophoresis. Edonerpic maleate significantly ($P < 0.05$) decreased the amount of monomeric CRMP2 (Fig. 1H), indicating that edonerpic maleate regulates multimerization of CRMP2 through direct interaction.

To examine whether CRMP2 mediates the edonerpic maleate–induced facilitation of synaptic AMPAR delivery in the adult mice barrel cortex, we used CRMP2-deficient mice (24). We administered edonerpic maleate as described above to 3-month-old CRMP2-deficient mice, measured the AMPA/NMDA ratio, and evoked mEPSC at layer 4–2/3 synapses onto pyramidal neurons of the barrel cortex. We observed a decreased

[1]Yokohama City University Graduate School of Medicine, Department of Physiology, Yokohama, 236-0004, Japan. [2]Human Informatics Research Institute, National Institute of Advanced Industrial Science and Technology, Ibaraki, 305-8568, Japan. [3]Toyama Chemical Co., Tokyo, 160-0023, Japan. [4]Fujifilm Corporation, Tokyo, 107-0052, Japan. [5]Yokohama City University Graduate School of Medicine, Department of Molecular Pharmacology and Neurobiology, Yokohama, 236-0004, Japan.
*These authors contributed equally to this work.
†Corresponding author. Email: takahast@yokohama-cu.ac.jp
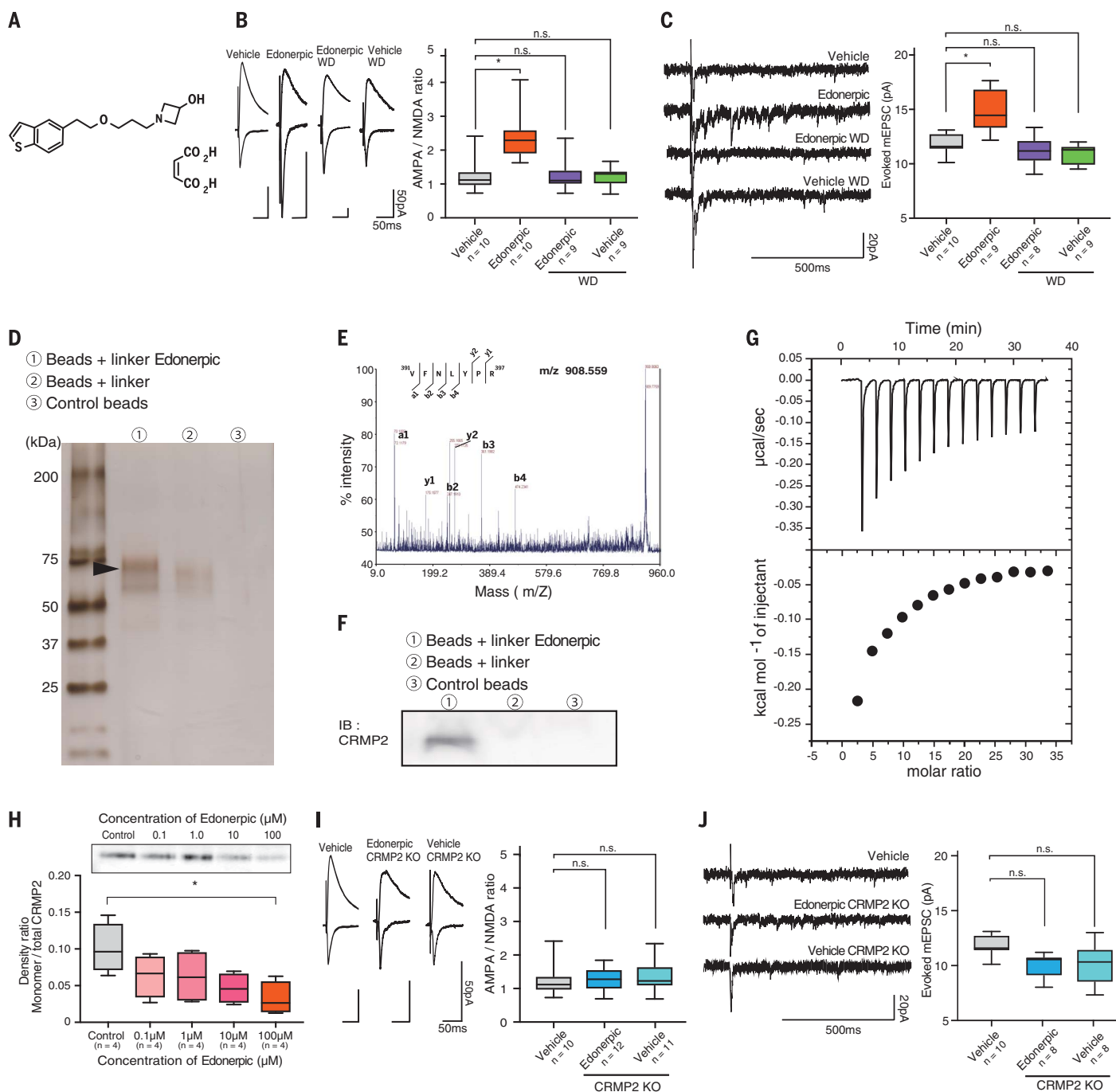
Fig. 1. Edonerpic maleate–induced facilitation of synaptic AMPAR delivery. (**A**) Chemical structure of edonerpic maleate. (**B**) (Left) Representative EPSCs in the barrel cortex treated with vehicle with intact whiskers, edonerpic with intact whiskers, edonerpic with whiskers deprived (WD), or vehicle with WD. (Right) Average AMPA/NMDA ratio. (**C**) (Left) Evoked mEPSC as in (B). (Right) Average amplitudes of evoked mEPSCs. (**D**) Silver-stained gel showing edonerpic-binding proteins. The black arrowhead indicates the protein selected for analysis with mass spectrometry. (**E**) Tandem mass spectra from tryptic digests of CRMP2. Fragment ions of the a, b, and y series identified in the tandem mass spectra from each peptide are shown. (**F**) Immunoblot of cortical lysate pulled down by indicated beads. (**G**) ITC-based measurements of

edonerpic fumarate binding to CRMP2. (Top) Raw thermogram. (Bottom) Integrated titration curve. (**H**) (Top) Immunoblot of purified CRMP2 reacted with edonerpic. (Bottom) Monomer-to–total CRMP2 ratio. Data were normalized to control. (**I**) (Left) Representative EPSCs in the barrel cortex in CRMP2 knockout mice. Data of WT mice treated with vehicle with intact whiskers were derived from Fig. 1B. (Right) Average AMPA/NMDA ratio. (**J**) (Left) Evoked mEPSC in the barrel cortex in CRMP2 knockout mice. Data of WT mice treated with vehicle with intact whiskers were derived from Fig. 1C. (Right) Average amplitudes of evoked mEPSCs. *$P < 0.05$. Data were analyzed with one-way ANOVA, with Dunnett's post hoc tests [(B), (C), (H), (I), and (J)]. The number of animals used for each experiment is indicated in the figure.

AMPA/NMDA ratio and the amplitude of evoked mEPSC in edonerpic maleate–administered CRMP2-deficient mice, compared with edonerpic maleate–administered wild-type (WT) mice, in the presence of whiskers [Fig. 1, I and J (and Fig. 1, B and C)]. The AMPA/NMDA ratio and the amplitude of evoked mEPSC in edonerpic maleate– or vehicle-administered CRMP2-deficient mice was comparable with that in vehicle-administered WT mice with whiskers and edonerpic maleate–administered WT mice in the absence of whiskers [Fig. 1, I and J] (and Fig. 1, B and C)]. There was no difference in kinetics of NMDAR-mediated currents among these groups (fig. S4C). We next knocked down the expression of CRMP2 of pyramidal neurons at layer 2/3 of the adult barrel cortex by means of lentivirus-mediated in vivo gene transfer of short hairpin RNA (shRNA) targeted to CRMP2 (25), examined the AMPA/NMDA ratio, and evoked mEPSC at layer 4–2/3 pyramidal synapses in the adult barrel cortex with whole-cell recordings. CRMP2 knockdown blocked edonerpic maleate–induced increase of the AMPA/NMDA ratio (fig. S4D) and the amplitude of evoked mEPSC at synapses formed from layer 4 to layer 2/3 pyramidal neurons (fig. S4E).

Edonerpic maleate accelerates motor function recovery from injury of the motor cortex

Recovery of motor function with rehabilitation after brain damage is considered to be a training-dependent plastic event in the nervous system. Edonerpic maleate, an enhancer of experience-dependent synaptic AMPAR delivery, could accelerate the effect of rehabilitation after brain damage of motor function recovery in a training-dependent manner. To assess this effect on forelimb movements, we trained mice to reach a forelimb for food pellets. Reaching forelimb movements were analyzed by the success rate of taking the food pellets (supplementary materials, materials and methods). As the mice were trained, the success rate improved (Fig. 2A). We first investigated whether the acquisition of the reaching task required synaptic AMPAR delivery. We overexpressed green fluorescent protein (GFP)–tagged cytoplasmic portion of GluA1 (a subunit of AMPA receptors) or GFP only in layer 5 of the motor cortex and trained animals in the reaching task. This peptide (GluA1-ct) prevents synaptic GluA1 delivery (12). Expression of GFP-GluA1-ct prevented acquisition of the reaching task, whereas GFP expression did not (fig. S5).

In humans, brain damage such as stroke disrupts once-acquired motor skills and leads to severe impairments. For the induction of brain injury, we used the cryoinjury method (supplementary materials, materials and methods). We trained animals in the reaching task and then induced motor cortical cryoinjury. Cryoinjury in the motor cortex of trained animals impaired their success rate (Fig. 2, B and C). After mild cortical cryoinjury, the decreased success rate in the reaching task could be recovered through training. This recovery was synaptic AMPAR delivery-dependent because expression of GFP-GluA1-ct in layer 5 of the intact motor cortex prevented recovery after training (fig. S6).

Next, we produced a more severe motor cortical cryoinjury (Fig. 2B) in trained animals. In this condition, training was not sufficient for recovery (Fig. 2C). One day after the injury, we initiated oral administration of edonerpic maleate (30 mg/kg, twice a day) or vehicle. Three weeks later, we treated mice with or without training. Training was initiated 1 hour after oral administration of edonerpic maleate, based on pharmacokinetic results, in which the maximum concentration of edonerpic was observed in the plasma and the brain in rodents at 1 hour after the oral administration (fig. S7). Concomitant training with edonerpic maleate administration dramatically recovered the impaired success rate in the reaching task. There was no obvious recovery in either edonerpic maleate–administered animals without training or vehicle-administered animals with or without training (Fig. 2D and fig. S8A). We also examined the dose-dependent effect of edonerpic maleate. One day after the injury, we started oral administration of edonerpic maleate in lower doses (20, 5, and 1 mg/kg, once a day). Three days later, we initiated training. Double-blind examination revealed that edonerpic maleate–administered mice at the dose of 20 or 5 mg/kg, but not 1 mg/kg, exhibited prominent recovery in reaching task performance in a rehabilitative training–dependent fashion (fig. S8B). We detected no significant difference ($P = 0.79$) of the injury size between vehicle-treated and edonerpic maleate–treated (20 mg/kg) mice during experiments (fig. S8C). Further, no behavioral abnormalities by the administration of edonerpic maleate have been observed (fig. S9). Neither SA4503 nor paroxetine, previously reported (26, 27) as potential accelerators of rehabilitation, showed effects on motor function recovery in this experimental design (fig. S10).

### Edonerpic maleate drives AMPARs into synapses of peri-injured regions

We next examined whether functional cortical reorganization is accompanied by edonerpic maleate–induced recovery after cryoinjury of the motor cortex. We produced the motor cortical cryoinjury and administered edonerpic maleate (30 mg/kg, twice a day) for three weeks, as described above, and trained animals for a week when we detected the motor function recovery. Then, we introduced a second lesion at the peri-injured region (just rostral to the first-injured region) (Fig. 2E). A week later, the animals with the second lesion exhibited deterioration of once-reacquired motor function compared with sham-operated animals (Fig. 2E). This indicates that edonerpic maleate–induced motor function recovery after cryoinjury results from functional reorganization of the cortex.

We examined whether synaptic AMPAR contents are altered by edonerpic maleate in the motor cortex of injured animals with recovered motor function. We produced the motor cortical cryoinjury and administered edonerpic maleate (30 mg/kg, twice a day) or vehicle for 3 weeks. Then, we treated animals with or without training and, 6 weeks later, prepared acute brain slices and recorded from layer 5 pyramidal neurons in the above detected peri-injured region of the motor cortex, which could compensate for lost cortical function (Fig. 2F). Edonerpic maleate–administered recovered animals exhibited increased amplitude of mEPSCs, compared with vehicle-administered unrecovered mice (Fig. 2F). Consistent with the dose-dependent effects of edonerpic maleate on motor function recovery, edonerpic maleate–administered mice at 20 or 5 mg/kg (recovered), but not 1 mg/kg (non-recovered), exhibited a prominent increase of the amplitude of mEPSC in the compensatory peri-injured region. In this experiment, 1 day after the injury, we started oral administration of edonerpic maleate at a reduced dose: 20, 5, and 1 mg/kg, once a day. Three days later, we initiated training. Four weeks after the start of training, we prepared acute brain slices and recorded from pyramidal neurons of layer 5 (fig. S11).

Next, we examined whether edonerpic maleate–induced recovery of motor function after cryoinjury of the motor cortex requires synaptic delivery of AMPARs in the cortical region, which was not primarily responsible for reaching task

Table 1. Monkeys used in the present study. Three monkeys were used in each treatment. There are no significant differences ($P = 0.2$ for weight, $P = 0.6$ for days of first reach) in body weight, age, or days of first reach.

	No.	Weight (kg)	Age (years)	Dominant hand	Days of first reach
Edonerpic	A	5.14	5	L	25
	B	4.94	5	R	8
	C	4.10	5	R	8
	Mean	4.73			13.7
Vehicle	D	4.41	5	L	9
	E	3.68	5	L	10
	F	4.05	6	R	12
	Mean	4.05			10.3
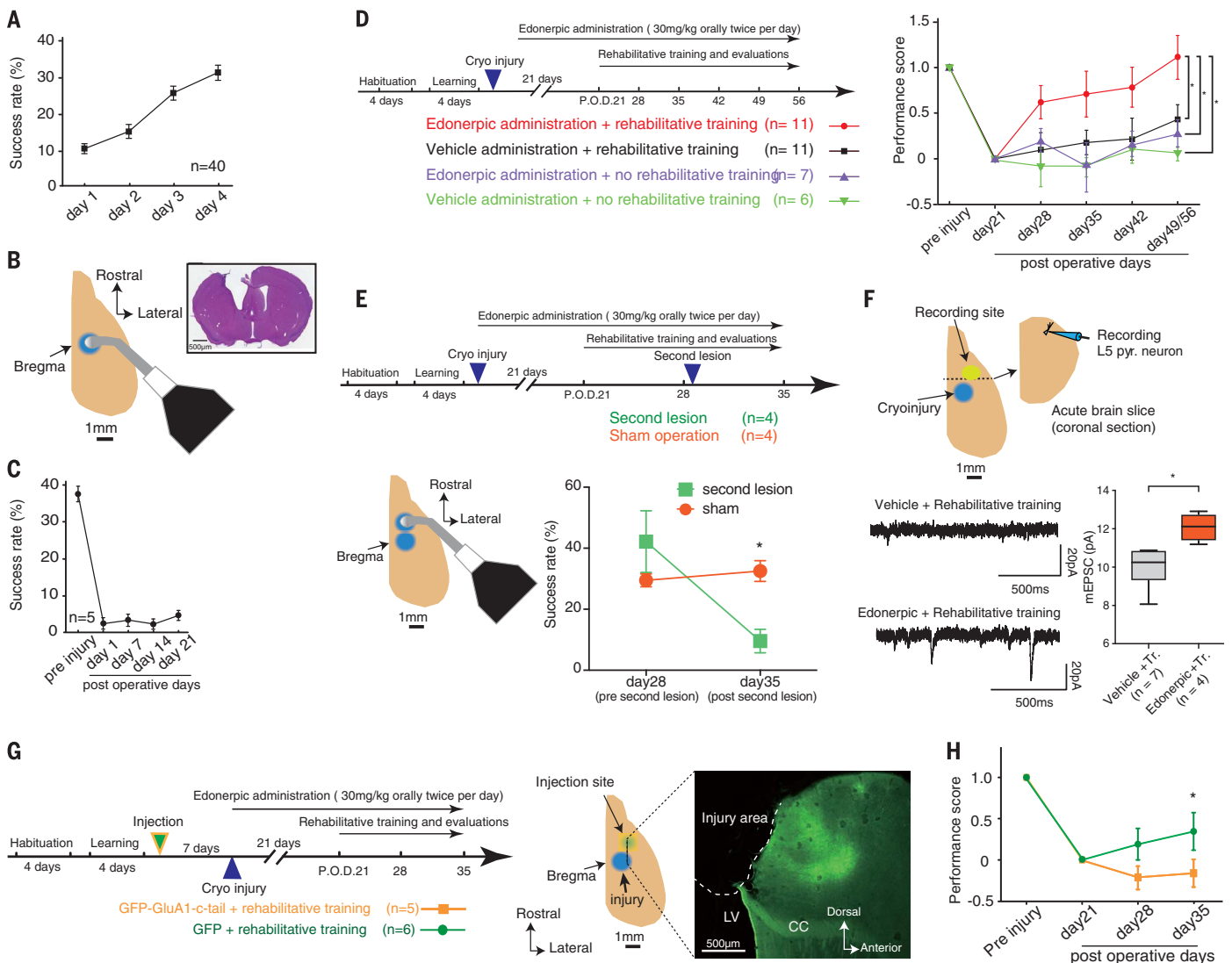
Fig. 2. Accelerated recovery of the motor function after functional cortical reorganization. (**A**) Average success rate (SR) in the reaching task. (**B**) (Left) Schema of cryoinjury. (Right) Hematoxylin-eosin−stained with severe cryoinjury. (**C**) Average SR after cryoinjury. (**D**) (Left) Experimental design of treatments. (Right) Average performance score (PS). (**E**) (Top) Experimental design for the evaluation with second lesion at the peri-injured cortex. (Bottom left) Schema of second lesion. (Bottom right) Average SR in day 28 (before second lesion) or 35 (after second lesion). (**F**) (Top) Representative mEPSC at layer 5 pyramidal neurons in the peri-injured region. (Bottom left) Representative mEPSC at layer 5 pyramidal neurons in the peri-injured cortex after day 56 [as in (D)].

Edonerpic with rehabilitative training or vehicle with rehabilitative training. (Bottom right) Average amplitudes of mEPSCs. (**G**) (Left) Experimental design for the evaluation with GFP-GluA1-ct or GFP expression by lentivirus in the peri-injured cortex. (Middle) Representative photomicrograph of the virus injection site. (Right) GFP-expressing cells in the peri-injured cortex. The dotted line represents the cryo-injured region. LV, lateral ventricle; CC, corpus callosum. (**H**) Average PS in mice with GFP-GluA1-c-tail or GFP expression. Data were analyzed with two-way ANOVA, followed by Bonferroni's post hoc tests in (D) and (H), or unpaired *t* test in (E) and (F). *$P < 0.05$. The number of animals used in each experiment is indicated in the figure.

performance before the cryoinjury. We trained animals in the reaching task and expressed GFP-tagged GluA1-ct or GFP in the motor cortex by means of lentivirus-mediated in vivo gene transfer (Fig. 2G). Injected areas were wider than injured areas and covered potential compensatory areas detected in the previous experiments (Fig. 2E). We then introduced cryoinjury in the motor cortex as described above. One day after the injury, we started oral administration of edonerpic maleate (30 mg/kg, twice a day). Three weeks after the initiation of edonerpic maleate administration,

we initiated the training. One week after the beginning of the training, we began evaluating the recovery of motor function in the reaching task. Expression of GluA1-ct prevented edonerpic maleate–induced recovery of motor function (Fig. 2H).

CRMP2 mediates edonerpic maleate–induced acceleration of motor function recovery through rehabilitative training

We found that edonerpic bound to CRMP2 (K_d = ~7.35×10^{-4} M). To examine whether
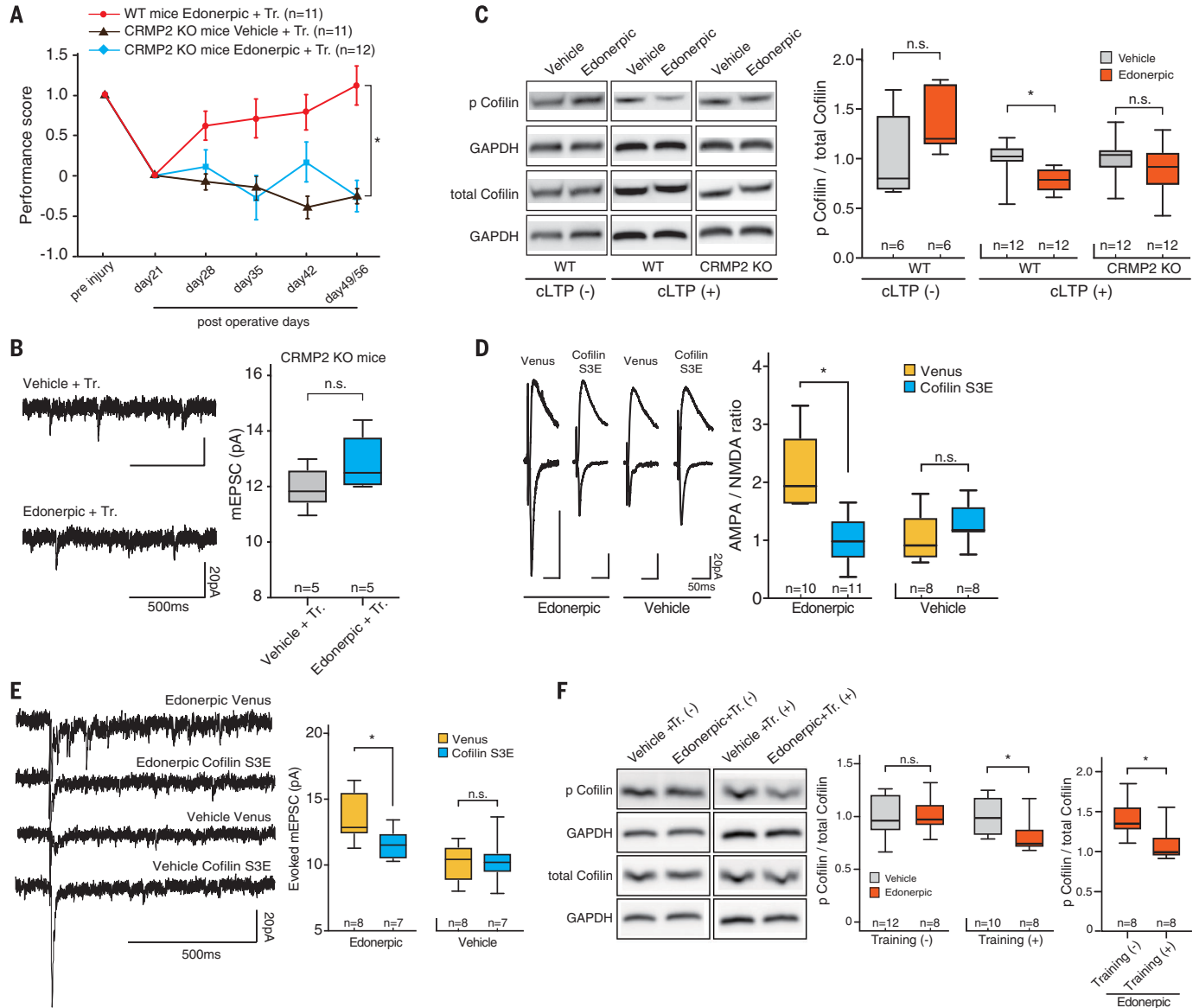
edonerpic maleate–induced functional recovery is mediated by CRMP2, we produced the motor cortical cryoinjury in trained CRMP2-deficient mice in the reaching task, as described above. After the injury, we orally administered edonerpic maleate (30 mg/kg, twice a day) or vehicle. Three weeks later, we treated mice with or without training. During the training period, we evaluated the reaching task of these mice once a week as in the experiments described above. Training failed to recover reaching task performance in the mutant mice treated with

edonerpic maleate (Fig. 3A and fig. S8A). Consistent with this behavioral experiment, we detected no increase in the amplitude of mEPSCs of layer 5 pyramidal neurons of intact compensatory peri-injured motor cortical region of edonerpic maleate–administration CRMP2-

deficient mice 6 weeks after the beginning of the training (Fig. 3B).

Because abnormal neurological conditions could modulate CRMP2 (20, 28), we investigated the phosphorylation status of CRMP2 in the compensatory peri-injured region from edo-

nerpic maleate–treated injured mice that recovered with rehabilitative training. We detected decreased amount of phosphorylated CRMP2 in edonerpic maleate–treated recovered mice than vehicle-treated unrecovered mice with training (fig. S12A).

Fig. 3. CRMP2 mediates edonerpic–induced functional recovery via ADF/cofilin activation. (**A**) Average performance score. WT mice data were derived from Fig. 2D. CRMP2 knockout data were added. (**B**) (Left) Representative mEPSC at layer 5 pyramidal neurons in the peri-injured region of CRMP2 knockout mice (Fig. 2F). Edonerpic + rehabilitative training (Tr.)/knockout or vehicle + Tr. / knockout. (Right) Average amplitudes of mEPSCs. (**C**) (Left) Immunoblots of Cofilin, phosphorylated Cofilin, and glyceraldehyde-3-phosphate dehydrogenase (GAPDH) obtained from cLTP-induced cortical slices of WT or CRMP2 knockout mice. (Right) The level of p-Cofilin. GAPDH was used as the reference. The data were normalized to the vehicle-treated group. (**D**) (Left) Representative EPSCs from Venus-expressing neurons or Cofilin S3E in the barrel cortex of mice administered with edonerpic or vehicle.

(Right) Average AMPA/NMDA ratio. (**E**) (Left) Evoked mEPSC as in (D). (Right) Average amplitudes of evoked mEPSCs. (**F**) (Left) Immunoblots of Cofilin, p-Cofilin, and GAPDH from peri-injured cortical region of mice at day 28 (Fig. 2D). (Middle) Phosphorylation level of Cofilin. GAPDH was used as the reference. The data were normalized to the vehicle-treated group. (Right) Phosphorylation level of Cofilin in the peri-injured regions of edonerpic maleate–administered mice (comparison between with and without training). GAPDH was used as the reference. Data were analyzed with two-way ANOVA, followed by Bonferroni's post hoc tests [(A); edonerpic + Tr. / WT versus other groups in day 35, 42, and 49/56], or unpaired t test [(B), (C), (D), (E), and (F)]. *$P < 0.05$. n.s. indicates not significant. The number of animals used in each experiment is indicated in the figure.

CRMP2 mediates edonerpic maleate–induced activation of ADF/cofilin

To further elucidate the mechanisms of how edonerpic-CRMP2 interaction modifies synaptic function under the plasticity-inducing condition (29), we performed biochemical studies with chemical LTP-induced cortical slices. We prepared cortical slices of the motor cortex and chemically induced LTP (cLTP) by briefly exposing the slices to the potassium channel blocker tetraethylammonium (TEA) (30). The actin-depolymerizing factor (ADF)/cofilin mediates AMPAR trafficking during synaptic plasticity (30–32); thus, we focused on this molecule as a potential downstream effector of edonerpic-CRMP2 interaction. ADF/cofilin is inactivated by phosphorylation and activated by dephosphorylation at the serine-3 (Ser^3) residue. To determine whether edonerpic-maleate activates ADF/cofilin in slices of the motor cortex under cLTP, we prepared the synaptoneurosome fraction from cLTP-treated acute motor cortical slices. We detected decreased phosphorylation of ADF/cofilin at Ser^3 in the edonerpic maleate–treated slices, compared with vehicle-treated ones, under cLTP but not under the normal condition, suggesting that ADF/cofilin is activated by edonerpic maleate under cLTP (Fig. 3C and fig. S12B). Edonerpic maleate–induced activation of ADF/cofilin under cLTP was abolished in slices from CRMP2-deficient mice (Fig. 3C and fig. S12B). Further, the phosphorylation of ADF/cofilin at Ser^3 was decreased in slices of WT mice than CRMP2-deficient mice in the presence of edonerpic maleate (fig. S12C). These results indicate that edonerpic maleate–induced activation of ADF/cofilin under cLTP is mediated by CRMP2.

To test whether the activation of ADF/cofilin mediates edonerpic-CRMP2–induced facilitation of synaptic AMPAR delivery, we overexpressed the dominant negative form of ADF/cofilin (S3E) together with Venus or Venus alone in the adult barrel cortex of edonerpic maleate–administered or vehicle-treated mice with lentivirus. Three weeks after the initiation of edonerpic maleate administration, we prepared acute brain slices and examined the AMPA/NMDA ratio and evoked mEPSC at layer 4–2/3 pyramidal synapses. We detected decreased AMPA/NMDA ratio and the amplitude of evoked mEPSC by the expression of ADF/cofilin S3E, compared with the expression of Venus alone, in edonerpic maleate–administered animals (Fig. 3, D and E). We detected no significant ($P > 0.20$) decrease of AMPA/NMDA ratio and the amplitude of mEPSC at layer 4–2/3 pyramidal synapses by the expression of ADF/cofilin S3E compared with the expression of Venus alone in vehicle-treated animals (Fig. 3, D and E).

Consistent with this, we found activation of ADF/cofilin (decreased phosphorylation of ADF/cofilin at Ser3) in the synaptoneurosome fraction obtained from the compensatory peri-injured region of edonerpic maleate–administered recovered mice compared with vehicle-treated nonrecovered mice (Fig. 3F). We also found significant ($P < 0.01$) decrease of the phosphorylation levels of ADF/cofilin in edonerpic maleate–treated animals with training than in those without training (Fig. 3F).

Edonerpic maleate facilitates motor function recovery after ICH in nonhuman primates

Stroke such as hemorrhage and embolism in the internal capsule leads to severe paralysis of motor functions. The severity and outcome of motor impairments depend on the degree of damage to this region (33–36). To further show that edonerpic maleate facilitates training-dependent recovery from brain damage, we used an internal capsule hemorrhage (ICH) model in nonhuman primates. We trained macaque monkeys in two different tasks. A simple reach-to-grasp task aimed at evaluating the performance in both reaching and gross grasping (Fig. 4A). In nonhuman primates and humans, development of the corticospinal tract correlates with improvement in the index of dexterity, particularly in the ability to perform precision grip, holding a small object between the thumb and index finger tips (37). In the vertical-slit task, the performance of dexterous hand movements, typical of primates, were evaluated (Fig. 4B).

After monkeys learned to perform the tasks, we injected collagenase to the hemisphere contralateral to the preferred hand, under magnetic resonance imaging (MRI)–stereotaxic guidance. MRI scanning confirmed hemorrhage in the internal capsule (Fig. 4C). The area of the hyperintense signal expanded at days 3 to 7 after injection and then decreased (fig. S13A). Thereafter, the residual hypointense area was almost stable until the end of the experiment, 6 months after injection (fig. S13B). The lesion in the internal capsule was also histologically confirmed after the behavioral experiment ended (fig. S13C). Although there was a tendency that the decrease of lesion area in edonerpic maleate–treated animals during experiment is smaller than vehicle-treated monkeys, we did not detect statistical significance (fig. S13D).

Before ICH, all animals smoothly performed both tasks, and they used precision grip in the vertical-slit task (movie S1). Immediately after ICH, flaccid paralysis of the contralateral forelimb, almost complete paralysis of the hand digits, and incomplete but severe paralysis of the wrist, elbow, and shoulder were observed. Forelimb motor functions then gradually recovered. Some of the monkeys showed mild paralysis of the contralateral hindlimb immediately after ICH, but the paralysis disappeared within a few days. Although the average stroke volume of edonerpic maleate–administered monkeys was higher than that of vehicle-administered monkeys, the difference between the two groups was not statistically significant ($P = 0.90$, Mann-Whitney U test) (Fig. 4D). All monkeys were able to move the elbow and shoulder joints 1 to 2 weeks after ICH. On the day when the monkeys first reached for the piece of apple, presented in each task, rehabilitative training began (Fig. 4E and Table 1).

The rehabilitative training was initiated 15 min after the administration of edonerpic maleate, based on the results of the pharmacokinetic study (fig. S14).

During rehabilitative training, the performance of the simple reach-to-grasp task gradually recovered in both the edonerpic maleate– and vehicle-administered monkeys (Fig. 4, F, G, H, and I; and figs. S15 and S16). Two-way analysis of variance (ANOVA) revealed significant ($P < 0.001$) effects of edonerpic maleate administration on the recovery of time to retrievals, compared with the vehicle-administered group, for both near and far locations (Fig. 4, F and G, and movies S2 and S3). Although the effect of edonerpic maleate was significant ($P < 0.005$) for both locations in the early phase, the effect was significant ($P < 0.001$) only for far location in the late phase of the rehabilitative training period (Fig. 4, H and I). Retrieval from the far location required more coordination of forelimb muscles, including the proximal and distal parts, as compared with the near location. In the vertical slit task, a significant ($P < 0.001$) effect of edonerpic maleate administration was found for recovery of both the success rate and the time to retrieval, throughout the rehabilitative training period (Fig. 4, J, K, and L; and figs. S15 and S16). The edonerpic maleate–administered monkeys frequently showed dexterous hand movements, including precision grip after the rehabilitative training period (Fig. 4M and movie S4). On the other hand, precision grip was rarely observed in the vehicle-administered monkeys after ICH (Fig. 4M and movie S4).

Discussion

Although medication during the acute phase of brain damage exhibits some effectiveness, there is no small compound–mediated intervention to enhance the effect of later rehabilitation after functional loss due to brain damage (38). Previous experiments have shown that motor cortical reorganization in the intact regions of a damaged brain is crucial for functional recovery (4, 6, 7, 29, 39, 40). Here, we found that edonerpic maleate, a CRMP2-binding compound, accelerates functional recovery after brain damage in a rehabilitative training-dependent manner, which induces functional motor cortical reorganization. Thus, edonerpic maleate could provide a pharmacological solution for unmet medical needs. Although many compounds exhibit some effectiveness on motor function recovery in rodents, most fail to prove their efficacy in primates. In this study, we proved the prominent effect of edonerpic maleate on training-dependent motor function recovery in primates. Thus, edonerpic maleate may be a strong candidate for a small compound to accelerate rehabilitative training–dependent motor function recovery after brain damage, such as stroke, in humans.

CRMP2 can bind to actin, and its regulator proteins, which is crucial for synaptic AMPAR delivery (20, 31, 41, 42). Among them, the activation of ADF/cofilin drives trafficking of
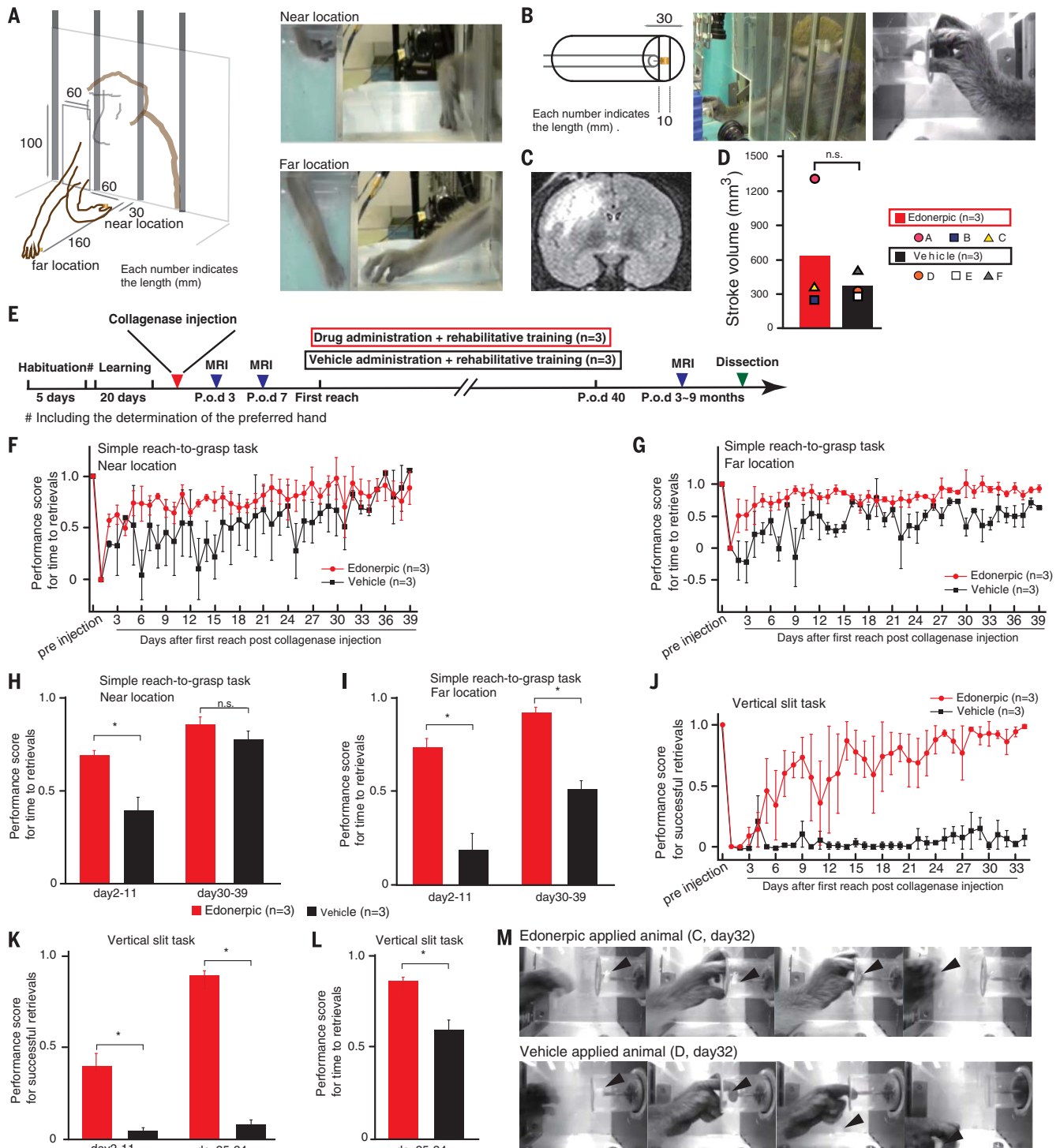
Fig. 4. Edonerpic maleate accelerates motor function recovery in nonhuman primates. (**A**) (Left) Simple reach-to-grasp task. (Right) Representative reaching and grasping for each location. (**B**) (Left middle) The vertical slit task. (Right) The finger-thumb grip in the vertical slit task before collagenase injection. (**C**) The fluid-attenuated inversion recovery images of MRI scanning (monkey D) 3 days after the collagenase injection into the right internal capsule. (**D**) Stroke volume of edonerpic maleate– or vehicle-administered monkeys. Each symbol indicates data from one monkey. There was no significant difference between the two groups (Mann-Whitney U-test, P = 0.90). (**E**) Experimental design. (**F** and **G**) Time course of the PS in the simple reach-to-grasp task. (**H** and **I**) Average PS in

the simple reach-to-grasp in the early (days 2 to 11) and in the late (days 30 to 39) phase of the training period. (**J**) Time course of the PS for successful retrievals in the vertical slit task. (**K**) The average PS in the vertical slit task in the early and in the late phase of the training period. (**L**) The average PS for time to retrievals in the late phase of the training period of the vertical slit task. (**M**) Sequential captures of the late phase (day 32) of the training period. Edonerpic maleate–administered monkeys could perform the task smoothly without dropping the piece of apple (black arrowheads indicate the apple's positions), whereas the vehicle-administered monkeys could not. Data were analyzed with two-way ANOVA [edonerpic-maleate, $P < 0.0001$; (F), (G), and (J)] and Mann-Whitney U-test [(H), (I), (K), and (L)]. $*P < 0.05$.

AMPAR into the spine surface under plasticity-inducing conditions (*31*). The activation of ADF/cofilin is involved in synaptic AMPAR trafficking in various genetic and environmental conditions (*30, 32*). We detected CRMP2-dependent activation of ADF/cofilin by edonerpic maleate in the plasticity-inducing condition. We also found that edonerpic CRMP2–induced activation of ADF/cofilin mediates the facilitation of synaptic AMPAR trafficking. CRMP2 is required for the trafficking of N-type voltage-sensitive Ca^{2+} channels (*43*). Thus, edonerpic-CRMP2 interaction could facilitate synaptic AMPAR delivery through the regulation of actin dynamics. In addition to actin dynamics, neuromodulatory systems such as dopaminergic and serotonergic inputs could regulate synaptic AMPAR trafficking (*15, 44*). It will be crucial to examine whether edonerpic-CRMP2 complex affects dopaminergic and serotonergic signaling.

Although the decrease of lesion area in edonerpic maleate–treated monkeys during experiment tended to be smaller than that in vehicle-treated monkeys, we did not detect statistical significance (fig. S13D). We also did not find any difference of the change of lesion volume during experiments between edonerpic maleate–treated and vehicle-treated mice (fig. S8C). Further, the recovery of edonerpic maleate–treated mice with cryoinjury was blocked by the expression of GluA1-ct in the compensatory cortical area (Fig. 2H). Taken together, edonerpic maleate–mediated facilitation of motor function recovery after brain injury is primarily mediated by the augmented synaptic AMPA receptor delivery. It will also be crucial to further study whether edonerpic maleate promotes neuroregeneration.

Although the affinity of edonerpic binding to CRMP2 was moderate (K_d = ~7.35 × 10^{-4} M), we found that (i) a major band specific to the sample that was pulled down with edonerpic-conjugated beads from the lysate of mice cortical primary culture corresponded to CRMP2 (there existed a faint band near CRMP2-positive bands with the edonerpic beadspulled-down preparation from CRMP2-deficient mice; this could be due to other isoforms of CRMP family), (ii) edonerpic maleate decreased the monomer of CRMP2 in the cell-free condition, (iii) edonerpic maleate–induced activation of ADF/cofilin in the plasticity-induced condition was blocked in the absence of CRMP2, (iv) edonerpic maleate–induced facilitation of synaptic AMPAR delivery was abolished in CRMP2-deficient mice, (v) edonerpic maleate–induced facilitation of synaptic AMPAR delivery was blocked by knocking down the expression of CRMP2 with shRNA, and (vi) edonerpic maleate–induced acceleration of motor function recovery was prevented in CRMP2-deficient mice. CRMP2 is an intracellular protein, and it is difficult to estimate the concentration of edonerpic maleate in the cortical neurons of treated animals. However, the evidence presented here suggests that CRMP2 is a primary target of edonerpic maleate for the rehabilitative training–dependent acceleration of motor function recovery from traumatic brain injury.

The efficacy of edonerpic maleate in humans should be evaluated in clinical trials because safety profiles of this compound have already been well established in clinical phase I studies. For stroke recovery, engineering technologies for rehabilitation, such as brain machine interface and robotics, are expected to be promising tools (*45, 46*). Other biological technologies, such as cell transplantation, may also be potential therapeutic alternatives, with distinct mechanisms from edonerpic maleate (*47*). Thus, the combination of these tools with the application of edonerpic maleate could induce synergistic effects and greatly increase the number of treatable patients with pathological brain damage.

REFERENCES AND NOTES

1. T. H. Murphy, D. Corbett, *Nat. Rev. Neurosci.* **10**, 861–872 (2009).
2. Y. Murata *et al.*, *J. Neurosci.* **35**, 84–95 (2015).
3. M. Nishibe, E. T. Urban 3rd, S. Barbay, R. J. Nudo, *Neurorehabil. Neural Repair* **29**, 472–482 (2015).
4. M. Nishibe, S. Barbay, D. Guggenmos, R. J. Nudo, *J. Neurotrauma* **27**, 2221–2232 (2010).
5. R. J. Nudo, *Curr. Opin. Neurobiol.* **16**, 638–644 (2006).
6. R. J. Nudo, *J. Commun. Disord.* **44**, 515–520 (2011).
7. R. J. Nudo, B. M. Wise, F. SiFuentes, G. W. Milliken, *Science* **272**, 1791–1794 (1996).
8. H. W. Kessels, R. Malinow, *Neuron* **61**, 340–350 (2009).
9. D. Mitsushima, K. Ishihara, A. Sano, H. W. Kessels, T. Takahashi, *Proc. Natl. Acad. Sci. U.S.A.* **108**, 12503–12508 (2011).
10. S. Rumpel, J. LeDoux, A. Zador, R. Malinow, *Science* **308**, 83–88 (2005).
11. D. Mitsushima, A. Sano, T. Takahashi, *Nat. Commun.* **4**, 2760 (2013).
12. T. Takahashi, K. Svoboda, R. Malinow, *Science* **299**, 1585–1588 (2003).
13. J. R. Whitlock, A. J. Heynen, M. G. Shuler, M. F. Bear, *Science* **313**, 1093–1097 (2006).
14. R. L. Clem, A. Barth, *Neuron* **49**, 663–670 (2006).
15. S. Jitsuki *et al.*, *Neuron* **69**, 780–792 (2011).
16. T. Miyazaki *et al.*, *J. Clin. Invest.* **122**, 2690–2701 (2012).
17. H. K. Lee *et al.*, *Cell* **112**, 631–643 (2003).
18. K. Takemoto *et al.*, *Nat. Biotechnol.* **35**, 38–47 (2017).
19. Y. Goshima, F. Nakamura, P. Strittmatter, S. M. Strittmatter, *Nature* **376**, 509–514 (1995).
20. K. Hensley, K. Venkova, A. Christov, W. Gunning, J. Park, *Mol. Neurobiol.* **43**, 180–191 (2011).
21. H. Nakamura *et al.*, *Genes Cells* **21**, 1059–1079 (2016).
22. K. Kadoyama *et al.*, *J. Neurosci. Res.* **93**, 1684–1692 (2015).
23. K. Hirata *et al.*, *J. Pharmacol. Exp. Ther.* **314**, 252–259 (2005).
24. H. Makihara *et al.*, *Genes Cells* **21**, 994–1005 (2016).
25. J. P. Ip *et al.*, *Nat. Neurosci.* **15**, 39–47 (2011).
26. K. Ruscher *et al.*, *Brain* **134**, 732–746 (2011).
27. F. Chollet *et al.*, *Lancet Neurol.* **10**, 123–130 (2011).
28. J. N. Zhang *et al.*, *Sci. Rep.* **6**, 37050 (2016).
29. R. J. Nudo, *Front. Hum. Neurosci.* **7**, 887 (2013).
30. H. Tada *et al.*, *Proc. Natl. Acad. Sci. U.S.A.* **113**, E7097–E7105 (2016).
31. J. Gu *et al.*, *Nat. Neurosci.* **13**, 1208–1215 (2010).
32. S. Jitsuki *et al.*, *Cereb. Cortex* **26**, 427–439 (2016).
33. S. K. Schiemanck, G. Kwakkel, M. W. Post, L. J. Kappelle, A. J. Prevo, *J. Rehabil. Med.* **40**, 96–101 (2008).
34. C. Rosso *et al.*, *Neuroradiology* **53**, 763–771 (2011).
35. R. Wenzelburger *et al.*, *Brain* **128**, 64–74 (2005).
36. Y. Murata, N. Higo, *PLOS ONE* **11**, e0154752 (2016).
37. G. Courtine *et al.*, *Nat. Med.* **13**, 561–566 (2007).
38. H. P. Adams Jr., R. J. Nudo, *Ann. Neurol.* **74**, 4–10 (2013).
39. S. Barbay *et al.*, *Stroke* **46**, 1620–1625 (2015).
40. R. J. Nudo, G. W. Milliken, W. M. Jenkins, M. M. Merzenich, *J. Neurosci.* **16**, 785–807 (1996).
41. K. Hensley *et al.*, *J. Neurosci.* **30**, 2979–2988 (2010).
42. Y. Kawano *et al.*, *Mol. Cell. Biol.* **25**, 9920–9935 (2005).
43. J. M. Brittain *et al.*, *Nat. Med.* **17**, 822–829 (2011).
44. D. S. Tukey, E. B. Ziff, *J. Biol. Chem.* **288**, 35297–35306 (2013).
45. M. D. Murphy, D. J. Guggenmos, D. T. Bundy, R. J. Nudo, *Front. Cell. Neurosci.* **9**, 497 (2016).
46. M. Aach *et al.*, *Spine J.* **14**, 2847–2853 (2014).
47. T. Yamashita *et al.*, *Cell Transplant.* **26**, 461–467 (2016).

Science

CRMP2-binding compound, edonerpic maleate, accelerates motor function recovery from brain damage

Hiroki Abe, Susumu Jitsuki, Waki Nakajima, Yumi Murata, Aoi Jitsuki-Takahashi, Yuki Katsuno, Hirobumi Tada, Akane Sano, Kumiko Suyama, Nobuyuki Mochizuki, Takashi Komori, Hitoshi Masuyama, Tomohiro Okuda, Yoshio Goshima, Noriyuki Higo and Takuya Takahashi

A small molecule for stroke therapy

Better therapies for motor impairments after stroke are greatly needed. In mice and nonhuman primates, Abe *et al.* found that edonerpic maleate enhanced synaptic plasticity and functional recovery after a traumatic insult to the brain (see the Perspective by Rumpel). This recovery of motor function was accompanied by functional reorganization of the cortex.

Science, this issue p. 50; see also p. 30

Supplementary Material for

CRMP2-binding compound, edonerpic maleate, accelerates motor function recovery from brain damage

Hiroki Abe, Susumu Jitsuki, Waki Nakajima, Yumi Murata, Aoi Jitsuki-Takahashi,
Yuki Katsuno, Hirobumi Tada, Akane Sano, Kumiko Suyama, Nobuyuki Mochizuki,
Takashi Komori, Hitoshi Masuyama, Tomohiro Okuda, Yoshio Goshima, Noriyuki Higo,
Takuya Takahashi*

*Corresponding author. E-mail: takahast@yokohama-cu.ac.jp

This PDF file includes:

Materials and Methods
Figs. S1 to S16
References

Other Supplementary Material for this manuscript includes the following:
(available at www.sciencemag.org/content/360/6384/50/suppl/DC1)

Movies S1 to S4

Supplementary Materials:

Materials and Methods

Figures S1-S16

Movies S1-S4

References (48-67)

Materials and methods for the rodent experiments

Ethics statement

All experiments were conducted according to the Guide for the Care and Use of Laboratory Animals (Japan Neuroscience Society) and the Guide for Yokohama City University and Toyama Chemical Co., Ltd. All animal experiments were approved by the Animal Care and Use Committee of Yokohama City University (authorization number: F-A-14-026). All surgical procedures were performed under anesthesia, and every effort was made to minimize the sufferings.

Animals

C57BL/6J male mice (18–25 g, 5 weeks of age) and CRMP2 knockout (KO) mice (18–25 g, 5–8 weeks of age) were housed on a 12-h light/dark cycle with *ad libitum* access to water and food. Procedures were performed in strict compliance with the animal use and care guidelines of Yokohama City University.

Reaching task

All behavioral experiments were performed under conditions of dim light (20–25 lux) in a silent room. Mice were habituated to the room for 1 h before every behavioral session. Mice were food restricted (1.5 g/day/animal) only one day before each session during the habituation, learning, and rehabilitative training periods, but water was provided *ad libitum*. The reaching task apparatus (8.5-cm width, 20-cm height, and 14-cm depth) was equipped with a 1.25-cm high food pellet stand. In addition, a 0.5-cm wide and 13-cm high slit was located at the bottom left of the apparatus (*48*). All mice were habituated to the apparatus over 4 days: Mice were allowed to move freely in the apparatus on the first day. On the subsequent days, pellets were placed in the apparatus (second day), both in the apparatus

and on the stand (third day), and only on the stand (fourth day). The learning period was initiated after the habituation was terminated. In the learning period, the pellet was placed diagonally in front of the slit to force the mice to use their left forelimb in each session. Each session consisted of either 30 trials or 20 min. Success was defined when mice were able to retrieving the pellet by a single reaching attempt without dropping it. Retrieving but dropping the pellet, reaching with many attempts, flipping the pellet, or using their right forelimb were defined as failure. The success rate was calculated as the number of success trials divided by the total number of trials.

Cryoinjury

After completing the motor learning phase of the reaching task, cryoinjury (*49*) was introduced into the mouse motor cortex using the Cryo system for ophthalmic surgery (Keeler Instruments). Briefly, mice were deeply anesthetized with isoflurane/oxygen mixture. The skin overlying the skull was cut and gently pushed to the side. The anterior fontanel was identified, and a region above the sensory-motor cortex (0.1 mm anterior to bregma, 2.1 mm lateral to bregma) (*50*) was gently pierced with trephine (diameter, 2.3 mm). A metal probe chilled with CO_2 gas was applied to the burr hole in cycles comprising a 30-sec application with one cycle for mild injury or two cycles for severe injury employed for each mouse. After surgery, the skin was repositioned and maintained with cyanoacrylate glue. Mice were kept on a heating pad during the procedures, and were returned to their home cages after regaining movement. To confirm the histological severity of cryoinjury, the hematoxylin-eosin staining was used.

Infection of cortical neurons *in vivo*

Mice were deeply anesthetized with an isoflurane-oxygen mixture. The skin overlying the skull was cut and gently pushed to the side. The anterior fontanel was identified, and a region above the target area was gently pierced with a dental drill. Lentivirus was pressure-injected through a pulled-glass capillary (Duramond). The injection coordinates for the intact motor cortex were 0 mm anterior to bregma (AP), 2.1 mm lateral to bregma (ML); 0.5 AP, 2.1 ML; and -0.5 AP, 2.1 ML; perilesional cortex (2.0 AP, 2.5 ML; 2.0 AP, 2.0 ML; 2.0 AP, 1.5 ML; 2.5 AP, 2.5 ML; 2.5 AP, 2.0 ML; and 2.5 AP, 1.5 ML); perilesional cortex (lateral part; -0.5 AP, 4.0 ML; 0 AP, 4.0 ML; 0.5 AP, 4.0 ML; 1.0 AP, 3.5 ML; and 1.5 AP, 3.5 ML); and barrel cortex (2.0 AP, 2.5 ML). Injections in the perilesional and motor cortices were at 1.0-mm depth, and barrel cortex at 0.3-mm depth. The injection syringe remained in place for 2 min after completion of each injection. After injection, the skin was repositioned and maintained with cyanoacrylate glue. Mice were kept on a heating pad during the procedures, and

returned to their home cages after regaining movement. For recordings of synaptic responses from cofilin S3E, Venus, short hairpin CRMP2 or scrambled ShRNA infected cells in the barrel cortex, virus infection was performed 1 week prior to edonerpic-maleate application.

Rehabilitative training

During the period of rehabilitative training, mice were placed in the apparatus for 30 min with some pellets on the stand in front of the slit so that they could reach the pellets by their affected forelimb.

Evaluation of motor functions

a. GFP-GluA1-ct and GFP mice (Fig. S5): The mice injected with lentivirus carrying GFP- GluA1 c-tail (ct) or GFP after the habituation period were trained to perform the reaching task for four days one week after the injection.

b. Cryo-injured mice (Fig. 2C): After the learning period and before the rehabilitative training, cryogenic injury was induced in mice (severe injury), which were tested at post-injury days 1, 7, 14, and 21.

c. GFP-GluA1-ct or GFP cryo-injured mice (Fig. S6): After the learning period, i.e., before the rehabilitative training period, lentivirus carrying GFP-GluA1-ct or GFP was injected. One week after the injection, the mice were cryo-injured (mild injury). Subsequently, mice were tested at post-injury days 1, 7, 14, and 21. Additionally, mice were subjected to a daily rehabilitative training starting from post-injury day 2 and continuing each day, except for the test days.

d. Cryo-injured mice treated with edonerpic-maleate or vehicle (Fig. 2D, 3A): After the learning period, mice were cryo-injured (severe injury; Fig. 2B) and subsequently received 30 mg/kg of edonerpic-maleate or vehicle orally twice a day starting from post-injury day 1 until the final test day. Mice were tested at post-injury days 21, 28, 35, 42, 49, and 56, and were subjected to a daily rehabilitative training starting from post-injury day 22, except for the test days.

e. Cryo-injured mice treated with 20, 5, or 1 mg/kg of edonerpic-maleate or vehicle (Fig. S8): The injured mice received 20, 5, or 1 mg/kg edonerpic-maleate or vehicle orally once a day starting from post injury day 1 until the final test day. Mice were tested at post-injury days 3, 10, 17, 24, and 31. They were additionally subjected to a daily rehabilitative training starting from post-injury day 4,

except for the test days. These tests were conducted under blinded conditions.

f. Cryo-injured mice treated with SA4503 or paroxetine (Fig. S10): The post-injured mice received 1 mg/kg SA4503, 10 mg/kg paroxetine, or the same volume of vehicle orally once a day starting from post-injury day 1 until the final test day. They were tested at post-injury days 3, 10, 17, 24, and 31. Additionally, they were subjected to a daily rehabilitative training starting from post-injury day 4, except for the test days.

g. Mice introduced second lesion in the rehabilitative training period (Fig. 2E): The injured mice received 30 mg/kg edonerpic-maleate orally twice a day starting from post injury day 1 to the final test day. They were tested at post-injury days 21 and 28. The recovered mice were, again, cryo-injured at day 29 as indicated in Figure 2E (just rostral to the first injured area), and subsequently tested at day 35. They were subjected to a daily rehabilitative training starting from post-injury day 22, except for the test and surgery days.

h. GFP-GluA1-ct or GFP mice treated with edonerpic-maleate in the rehabilitative training period (Fig. 2G): After the learning period, lentivirus carrying GFP-GluA1-ct or GFP was injected. One week after the injection, mice were cryo-injured (severe injury). Subsequently, mice received 30 mg/kg edonerpic-maleate or vehicle orally twice a day starting from post-injury day 1 to the final test day. They were tested at post-injury days 21, 28, and 35. Additionally, mice were subjected to a daily rehabilitative training starting from post-injury day 22, except for the test days.

Calculation of the performance score

The performance score (PS) was calculated using the following equation: *PS = (Success rate at day X – Success rate at first evaluation day after injury) / (Success rate at 4th learning day before injury – Success rate at first evaluation day after injury).* The value of 1 corresponded to pre-injury and 0 to the first evaluation day after injury in each mouse. This calculation made it possible to compare the recovery of mice with different severities.

Food consumption test

To test the effects of edonerpic-maleate on the feeding behavior, food consumption was measured. After handling for 3 days, mice were orally administered with 30 mg/kg of edonerpic-maleate or vehicle twice a day for 3 days. Soon after the final administration, weight-measured food was given.

On the subsequent day, the weights of the residual food were recorded.

Open field test

To test locomotor activity and anxiety-like behavior, the open field test was conducted as described previously (*51*). Prior to the test, mice received 30 mg/kg of edonerpic-maleate or vehicle orally twice a day for 3 days. During the test, a mouse was placed at the corner of the test chamber ($50 \times 50 \times 40$ cm^3; O'Hara & Co., Ltd, Tokyo, Japan) with 70 lux of lightning condition. All the mice behaviors were recorded during 1 h. The activity in the test chamber was tracked and analyzed using an imaging software (O'Hara & Co., Ltd).

DNA constructs

GFP-tagged GluA1-ct (*52*) was subcloned into pFUGW vector (lentivirus vector) using EcoR1/BamHI restriction enzyme. Lentivirus carrying GFP-GluA1-ct was produced as previously described (*16*). For the expression of the dominant-negative form of cofilin (cofilin S3E), the cofilin S3E was subcloned into the CSII-EF-MCS-IRES-VENUS vector using Not1. The cofilin S3E-IRES2-Venus was subcloned into the pFUGW vector using EcoR1 and BamH1. The short hairpin constructs were generated using the pLenti-Lox 3.7 vector. The CMV promoter of pLenti-Lox 3.7 was replaced with the CaMKII promoter using Not1/Nhe1. The following oligonucleotides were annealed with their complimentary sequences and inserted into the Hpa1 sites of pLenti-Lox3.7: short hairpin CRMP2 (ShCRMP2) (*25*) GCAGTGCTCTTGAGTACAAC, scrambled ShRNA (SCR) TGCATTCTCTAAGCCAACG. For the synthesis of full-length human CRMP2, the plasmid encoding human CRMP2 was kindly provided by Dr. Goshima. CRMP2 was subcloned into pGEX 6P-1 vector using Bgl2/EcoR1 restriction enzyme. GST-CRMP2 cDNA was subcloned into the MCS of pEU-SP6-E01 vector (vector for protein synthesis, Cell Free Science) using restriction enzyme Spe1/Kpn1. All constructs were confirmed through DNA sequencing.

Synthesis of GST-CRMP2

The GST-CRMP2 protein was synthesized by wheat germ cell-free expression system using WEPRO7240 (Cell Free Science). The GST-CRMP2 protein was incubated with PreScission protease (GE Healthcare) at 4°C overnight to cleave the GST tag. CRMP2, GST, and nucleic acid fractions were obtained by gel filtration chromatography with AKTA Purifier (GE Healthcare). These fractions were subjected to measurement using isothermal titration calorimetry.

Preparation of the cytosolic fraction from cortical neurons

Cortical neurons derived from embryonic day 16 (E16) brains of C57BL/6J mice and CRMP2 KO mice were plated at a density of 1×10^7 cells/dish in 6-cm dishes that were coated with poly-L-lysine and grown in Dulbecco's Modified Eagle Medium (DMEM) containing 10% fetal bovine serum (FBS), and 2 mM glutamine. Forty-eight hours after cell seeding, 10 μM cytosine arabinoside were applied to the cultures for 24 h. After 7 days in culture, cortical neurons were harvested with cell lysis buffer (20 mM Tris pH 7.4, 2 mM ethylenediaminetetraacetic acid [EDTA], 2 mM ethylene glycol-bis[β-aminoethyl ether]-N,N,N′,N′-tetraacetic acid [EGTA], protease inhibitor cocktail, and 1 mM DTT). The cell lysates were centrifuged at 100,000 ×*g* for 60 min at 4°C. The cytosolic fractions from the lysates were subjected to ligand-based target fishing.

Preparation of chemical long-term potentiation (LTP) induced brain slices

Brains of 7–8-week-old mice were rapidly extracted and quickly transferred into a dissection buffer. Subsequently, coronal brain slices were cut (400 μm, Leica VT1000) as in the electrophysiology protocol. These slices were incubated in gassed artificial cerebrospinal fluid (ACSF) containing 118 mM NaCl, 2.5 mM KCl, 4 mM $CaCl_2$, 4 mM $MgCl_2$, 26 mM $NaHCO_3$, 1 mM NaH_2PO_4, and 10 mM glucose (*16, 51*) with 10 μg/mL edonerpic for 3 h at room temperature. After edonerpic incubation, the slices were transferred into 38°C gassed ACSF with 25 mM TEA for 10 min. Subsequently, the slices were transferred into 38°C gassed ACSF for 30 min to wash out TEA. Finally, the cortex was trimmed from the slices in ACSF on iced plate and stored in liquid nitrogen.

Preparation of peri-injured cortex from cryogenic injured mice

Mice brains were rapidly extracted within 10 min after motor function evaluation at post-injury day 28 and were quickly transferred into the dissection buffer. The brains were gently put on a rodent brain matrix (ASI instrument) and sliced to 2-mm thick blocks. The slices including the injury site were selected and the cortex was trimmed within 1 mm from the injury site, which included the recording site (Fig. 2F). The trimmed cortex was stored in liquid nitrogen.

Preparation of synaptoneurosome fractions

Frozen samples were homogenized in ice-cold homogenization buffer A (10 mM HEPES, 1.0 mM EDTA, 2.0 mM EGTA, 0.5 mM DTT, 0.05 μM microcystine, 0.1 mM PMSF, 5 ng/μL leupeptin, 1% phosphatase inhibitor, and 2% protease inhibitor). The tissue was homogenized in a glass/glass tissue homogenizer. Homogenates were passed through two 100-μm-pore nylon mesh filters, and then

through a 5-µm-pore filter. Filtered homogenates were centrifuged at 14,400 rpm for 5 min at 4°C (*16*). The resultant pellets were resuspended in 100 µL boiling 1% sodium dodecyl sulfate (SDS), boiled for 10 min, and stored at −80°C.

Affinity purification

To identify the edonerpic-interacting protein from cortical neurons, a carrier compound composed of resin (TOYOPEARL AM-amino-650M), linker, and edonerpic structure was synthesized (Edonerpic-beads, Figure S4A). Two types of other carrier compounds without most of the edonerpic structure (Linker-beads, Control beads; Fig. S4A) were also synthesized and used as controls. The carrier compounds were suspended in cell lysis buffer, and were put into a blank column attached to the 10 µm pore filter. The carrier was washed, and the cytosolic fractions of the lysates were loaded into the column to interact with the carrier. Subsequently, the protein-carrier complex was competitively eluted with washing buffer containing 100 mM of edonerpic. The eluted fraction was concentrated by ultrafiltration (3 kDa cutoff), and denatured at 100°C for mass spectrometry (MS).

Mass spectrometry

The eluted proteins were separated by SDS-PAGE and stained with Protein Silver Stain Kit II (Wako, Tokyo, Japan). Protein bands around 60 kDa were excised from silver-stained gels, de-stained, and subjected to in-gel digestion overnight at 37°C with 5 ng/µL endoproteinase Glu-C (Sigma) or 12.5 ng/µL trypsin (Promega) in 25 mM ammonium bicarbonate. For the analysis on a MALDI-TOF/TOF MS (4800 Proteomics Analyzer, AB SCIEX), the resulting peptides were desalted using a Stage Tip-C18 (*53*) and then eluted directly onto a target plate with matrix solution containing 4 mg/mL CHCA (Sigma). The obtained MS and tandem-MS data were searched against the mouse protein sequences in the Uniprot/Swiss-Prot database (version Jan 2014) using the MASCOT software, version 2.5.1 (Matrix Science). The search parameters were as follows: three missed cleavages permitted; variable modifications: Carbamidomethylation, oxidation of methionine, and propionamidation of cysteine; peptide mass tolerance for MS data, ±0.06 Da; and fragment mass tolerance, ±0.065 Da. For the evaluation of the database-search results using MASCOT, "bold red" peptides with a peptide score ≥ 25 were considered as evaluation peptides. Proteins that had a protein score ≥ 35 were accepted as positive identifications in MALDI-TOF/TOF MS.

Isothermal titration calorimetry

Full length CRMP2 protein, GST protein, and nucleic acid fraction were dialyzed using 50 mM

HEPES. Dialysis extra fluid were used to adjust the concentration of each fraction and edonerpic-fumarate (full length CRMP2 50 μM, GST proteins 30 μM, edonerpic-fumarate 3 mM for titration of GST and nucleic acid, 8 mM for titration of full length CRMP2). Isothermal titration calorimetry performed by MicroCal iTC200 (Malvern). The measuring parameters were described below. Temperature and reference power were 25°C and 5 μcal/sec, respectively. A total of 14 injections with an initial delay of 60 sec for each titration were performed with constant stirring speed 1,000 rpm. The first injection of 0.2 μL over a time period of 0.4 sec was followed by 13 injections of 3 μL over 6 seconds each spaced by 150 sec. Integrated data were plotted using included software of the device, edonerpic-fumarate, and full length CRMP2 binding data were fitted to Low-C model to estimate K, enthalpy (ΔH) and entropy (ΔS). Changes in free energy (ΔG) were calculated using Gibbs equation, $\Delta G = \Delta H - T\Delta S$. Furthermore, Kd was calculated with reciprocal K.

Native polyacrylamide gel electrophoresis (native PAGE)

A total of 1.5 mg/mL purified GST-CRMP2 (2 μL) was incubated with PreScission protease (1 μL, GE Healthcare) in 20 mM Tris buffer (pH 7.4) at 4°C for 4 h. Subsequently, 1 μM, 10 μM, or 100 μM edonerpic or maleic acid were added as control sample with 20 mM Tris buffer (pH 7.4) and incubated at 4°C for 1 h. These reactant protein solutions were stirred with Native Page Sample Prep Kit (Thermo Fisher Scientific) including Native Page 4× sample buffer, 10% n-dodecyl-β-D-maltoside, 20 mM Tris-HCl (pH 7.4), Sample Marker, 5% G-250 solution and incubated for 45 min. These protein solutions samples and sample marker were loaded in each well and separated using 4–16% gradient gel for native PAGE. The cathode buffer included 10 mL 20× Native PAGE Running buffer (Life Technologies), 10 mL 20× Native PAGE Cathode buffer, which included G-250 (Invitrogen), and 180 mL deionized water. The anode running buffer included 30 mL of 20× Native Page Running buffer and 570 mL deionized water. Electrophoresis was continued at constant voltage (150 V) for 75 min on ice. After electrophoresis, separate sample markers were stained with Coomassie brilliant blue (CBB). For CBB staining, a marker lane of the gel was immersed in deionized water and warmed for 30 sec in the microwave oven, then shaken for 15 min. After disposing of the deionized water (40% methanol, 10% acetic acid), gel was put into de-staining water (8% acetic acid) overnight and scanned. Separated protein solution was transferred onto a PVDF membrane (Millipore) and blotted. For western blotting, separated protein lanes of the gel was denatured with SDS solution for 10 min at room temperature (20 mM Tris-HCl [pH 7.4], 150 mM Glycin, 0.1% SDS, and deionized water) and washed with transfer buffer for 5 min. Subsequently, the protein solutions were transferred onto the PVDF membrane in transfer buff at constant current (0.35 A) for 1 h on 4°C. To remove the residual

G-250, the membrane was washed with 8% acetic acid, then with Tris-buffered saline-tween (TBS-T) 10 minutes at room temperature 5 times. The membrane was blocked for 1 h in 4% skim milk (Yuki Jirushi Megmilk) at room temperature.

Western blotting

Samples were processed using 4–15% gradient gel (Biorad) and transferred to PVDF membranes. Membranes were blocked with 1% blocking buffer (Perfect-block; MoBiTec) in TBS-TritonX (0.1%) for 1 h and incubated overnight at 4°C with primary antibodies: anti-CRMP2 (Wako; 9F) at a 1:1000 dilution, anti-cofilin (Abcam; ab42824) at 1: 2000, anti-phosphorylated cofilin at 1: 2000 (Abcam; ab12866), and anti-GAPDH (Cell signaling technology; 14C10) at 1: 2000. Blots were subsequently washed in TBS-TritonX and placed in HRP-conjugated anti-rabbit secondary antibody at a 1:1000 dilution. After washing, blots were reacted with ECL or ECL-prime reagents. ECL-treated blots were quantified by densitometry using LAS4000 (Fujifilm). For quantification of CRMP2 phosphorylation, we recognized upper band as phosphorylated CRMP2 (*54, 55*).

Electrophysiology

After edonerpic-maleate treatment (for recording from layer 2/3 cells in the barrel cortex) or edonerpic-maleate treatment with rehabilitative training (for recording from layer 5 cells in the peri-injured cortex), mice were anesthetized with an isoflurane-oxygen mixture, and the brain was removed. The brain was quickly transferred into gassed (95% O_2 and 5% CO_2) ice-cold dissection buffer as described previously (*15*). Coronal brain slices were cut (350 μm, Leica VT1000) in the dissection buffer. The slices were then incubated in ACSF. Patch recording pipettes (3–7 MΩ) were filled with intracellular solution as described previously (*15, 16, (56*). For recording of AMPA/NMDA ratio in the layer 2/3 of the barrel cortex, the recording chamber was perfused with ACSF containing 0.1 mM picrotoxin, 4 μM 2-chloroadenosine, at 22–25°C. Whole-cell recordings were obtained from layer 2/3 pyramidal neurons of the mouse barrel cortex with a Multiclamp 700B (Axon Instruments). Bipolar tungsten stimulating electrodes were placed in layer 4. The stimulus intensity was increased until a synaptic response of an amplitude > 10 pA approximately was recorded. AMPA/NMDA ratios were calculated as the ratio of the peak current at -60 mV to the current at +40 mV after 50 ms stimulus onset (40–50 traces averaged for each holding potential), without D, L-APV in the recording chamber. To avoid stimulating the same sets of synapses when recording from distinct neurons, we picked up neurons from different barrel columns. To record the asynchronous quantal AMPAR-EPSCs (Sr^{2+}-mEPSCs) in the layer 2/3 of the barrel cortex, the recording chamber was perfused with Sr^{2+}-

containing ACSF as described previously (*56*). Bipolar tungsten stimulating electrodes were placed in layer 4. The detection threshold for Sr^{2+}-mEPSCs was set at 2X RMS noise. Asynchronous synaptic events were picked up from events that occurred between 200 and 2,000 ms after the stimulation. For recording of miniature AMPAR-EPSCs (mEPSCs) in the layer 5 of peri-lesional cortex, sections corresponding to Figures 11–19 in Franklin & Paxinos MOUSE BRAIN 3rd edition were selected. The recording chamber was perfused with 0.5 µM tetrodotoxin (TTX)-containing ACSF as described previously (*11*). The detection threshold for mEPSCs was set at 2× RMS noise.

In experiments analyzing facilitation of LTP in slices from adult wild-type mice were maintained in ACSF as described above. The slices were incubated in ACSF containing edonerpic-maleate (10 µg/mL) for at least 10 min. In order to monitor synaptic transmission, EPSC was evoked at 0.33 to 0.1 Hz and recorded at −60 mV holding potential in voltage-clamp mode. LTP was induced by a pairing protocol consisting of presynaptic fiber stimulation at 1 Hz for 180 sec paired with postsynaptic depolarization at -40 mV holding potential. Recordings were maintained for at least 40 min after pairing. The EPSC amplitude throughout the recording was always normalized to the average baseline amplitude before pairing.

All data for electrophysiology were analyzed using Clampfit 10.2 (Molecular Devices) or Mini analysis program 6.0.7 (Synaptosoft).

Pharmacokinetics profiles after single oral administration of edonerpic-maleate to mice

The pharmacokinetics study was conducted in Toyama Chemical Co., Ltd. Animals were anesthetized at the sampling time point; 0.083, 0.25, 0.5, 1, 2, 3, 5, 8, or 24 h after oral administration of edonerpic-maleate at doses of 10, 20, or 30 mg/kg or 0.083, 0.25, 0.5, 1, 2, 4, or 6 h after oral administration of edonerpic-maleate at 30 mg/kg. The samples were cooled on ice immediately and centrifuged (approximately 12,000 rpm) for 10 min at 4 °C (KUBOTA6200) within 1 h after the blood collection to separate the plasma samples. The obtained plasma samples were stored in a freezer (set to maintain −40°C). The measurement of plasma samples was performed on the few days following the blood collection. Quantification of edonerpic was performed by LC/MS/MS. Briefly, 50 µL samples were deproteinized using 100 µL of acetonitrile and analyzed using an LC/MS/MS system (LC, ACQUITY UPLC, Waters; MS/MS, TSQ Quantum Ultra Thermo Fisher Scientific) using a Waters 2.1 mm × 50 mm ACQUITY UPLC BEH C18 reverse phase column with a gradient program of 0.1% formic acid and acetonitrile/methanol (1:1, v/v). MS/MS detection was performed using single reaction monitoring (m/z 292 to 161 for edonerpic). Standard curve range of edonerpic was 1 to 500 ng/mL in plasma.

Statistics and graphs for rodent experiments

We performed statistical analysis using the number of animals as the number of observations (n=animals). For cell biological experiments, we averaged observations from experiments of one animal. Thus, we used the average of observations from one animal as n=1. To choose the appropriate statistical tests, the skewness and kurtosis of a sample distribution were calculated. If the skewness was less than 2 and kurtosis was less than 7, we analyzed the data using parametric tests. While the data showed that either skewness was more than 2 or kurtosis was more than 7, we used non-parametric tests (*57, 58*). As parametric tests, an unpaired two tailed t-test was used to compare two independent groups and an one-way ANOVA with post hoc Dunnett's test was used to compare more than three groups. As non-parametric tests, a Mann-Whitney U-test was used to compare two independent groups and a Kruskal-Wallis test followed by post hoc Dunn's test was used to compare more than three groups. If there were small number of samples (n≦3), non-parametric test was used. For analysis of time-dependent changes of reaching performance, two-way ANOVA followed by post hoc Bonferroni's test was used. $p < 0.05$ was considered statistically significant. Statistical analyses were conducted using GraphPad Prism 7 (Graph Pad Software) or SPSS software (SPSS 22.0; IBM). In the box plot graphs, the ends of the whisker were defined by maximum and minimum values. Central rectangles spanned from first quartile to third quartile. The segment in the rectangle indicated median. In the graph except for the box plot graphs, the error bars indicated standard error of the mean.

Materials and methods for the non-human primate experiments

Animals

Six male cynomolgus macaques (*Macaca fascicularis*, 3.68–5.14 kg, 5 or 6 years in age) were randomly assigned to two groups, edonerpic-maleate- and vehicle (Table 1). The macaques were bred and raised at Tsukuba Primate Research Center, National Institute of Biomedical Innovation (Ibaraki, Japan). No statistical methods were used to pre-determine the sample sizes. We attempted to minimize the number of monkeys used on the basis of ethical considerations and data similarity; our sample sizes were similar to those reported in previous publications by our group and others. Naive macaques without any history of experimentation were used. The animal use protocol was approved by the Institutional Animal Care and Use Committee of the National Institute of Advanced Industrial Science and Technology (AIST), Japan, and the Corporation for Production and Research of Laboratory

Primates, Japan conformed to the NIH Guidelines for the Care and Use of Laboratory Animals. The macaques were housed in adjoining individual primate cages allowing social interactions under controlled conditions of humidity, temperature, and light; they were monitored daily by the researchers and animal care staff to ensure their health and welfare. The housing area was maintained on a 12-h light/dark cycle, and all the experiments were conducted during the light cycle. A commercial primate diet and fresh fruit and vegetables were provided daily, and water was provided through an automatic watering system furnished to each cage. All efforts were made to minimize pain and discomfort of the animals throughout the course of the study.

Collagenase injection

We first determined the preferred hand of macaques by recording the hand that was used for reaching and grasping the target object, as in our previous studies (*59, 60*). We then injected collagenase type IV (C5138, Sigma, St. Louis, MO) into the posterior internal capsule of the hemisphere contralateral to the preferred hand. The location of the posterior internal capsule where the fibers from the M1 hand area descend was identified by using anatomical structures such as the central sulcus, thalamus, caudate nucleus, and putamen on the basis of data from anatomical tracer studies (*61, 62*). The anatomical structure of each macaque's brain was visualized on magnetic resonance images (MRI) obtained by using a 3-T MRI system (MAGNETOM Allegra; Siemens Medical Systems). Before the scan, the animals were anesthetized with isoflurane anesthesia and fixed into a magnet-free stereotactic frame. The imaging protocols consisted of a T1-weighted images, repetition time (TR) / echo time (TE), 2500 / 3.9 ms; number of excitations (NEX), 256 × 232; flip angle, 8°; field of view, 119 mm × 191 mm; matrix, 160 × 256; slice thickness, 0.7 mm. A MRI-based navigation system (Stealthstation TRIA plus; Medtronic) was used to determine the location of injection. A craniotomy was made over the internal capsule under sterile conditions and isoflurane anesthesia (0.8–1.5%), and collagenase type IV (200 units/mL in saline) was then injected via a Hamilton microsyringe (Hamilton Co.). A total of 9 injections were performed at three injection sites, separated by 1 mm in a dorsoventral direction, in each of three rostral–caudal tracks, which were also separated by 1 mm. The injection sites were centered at the identified stereotaxic coordinates for the posterior internal capsule where the motor tracts from the hand area of M1 descend. At each injection site, 3 μL collagenase was injected over 3 min.

Behavioral assessment after collagenase injection

Performance of hand movements before and after the collagenase injections was evaluated daily by

means of two different tasks; the simple reach-to-grasp task and the vertical-slit task (Fig. 4A, B). The simple reach-to-grasp task aimed to evaluate the performance of both reaching and gross grasping. In the task, the monkeys passed the hand through the rectangle hole at the corner of Plexiglas wall installed in front of the monkeys' cage, and then reached to and grasped a piece of apple ($7 \times 7 \times 7$ mm in size) placed at one of two places, near and far locations (Fig. 4A). In order to promote the use of the preferred hand, which had been determined by almost the same procedure as used in our previous studies (*59, 60*), the rectangle hole was located in the side of the monkey's preferred hands (Fig. 4A). Twenty pieces were placed on each of the two locations in the single session. In the vertical-slit task, the piece of apple ($7 \times 7 \times 7$ mm in size) was positioned in the center of a slit (30 mm in height and 10 mm in width) located at the shoulder height and at the sagittal distance of 15 cm from the cage (Fig. 4B). The Plexiglas wall with the rectangle hole at the corner was also installed in front of the slit to promote use of the preferred hand (Fig. 4B). This task was almost identical to the one used in our previous studies (*59, 63*), and 20 pieces were positioned in the single session. For both tasks, the macaque's movements were recorded by four video cameras (for simple reach-to-grasp task, one GZ-E565, JVC, Kanagawa, Japan; two HC-V750M, Panasonic; one WAT-902H Ultimate cameras, Watec; for vertical slit task, one HC-V750M, Panasonic; three WAT-902H Ultimate cameras) installed around the task apparatus. Behavioral assessments to evaluate functional recovery of forelimb movements began on the next day of the day when the monkey first reached for a food pellet positioned outside the cage using the affected hand. During the behavioral assessment, the monkeys were subjected to both the simple reach-to-grasp task and the vertical-slit task as described previously. One day after the monkey first reached for the piece of apple presented in each task, the post-lesion training started (Table 1). In the post-lesion training, the monkey underwent 30 trials for both tasks at 15 min after injection of edonerpic (15 mg/mL in 5% glucose solution, Otsuka Pharmaceutical Co) or vehicle (5% glucose solution). Since the blood concentration of edonerpic was highest at 20 min after the injection and gradually declined to the base line level within 6 h, we performed the rehabilitation during 15 min to 1 h after injection.

Movie analysis and calculation of the performance score

Analysis of simple reach-to-grasp task for near and far location

The recorded movies were analyzed by the software (Final Cut ProX ver.10.2.3, Apple Inc,). The frame rate of the recorded movies was 33 frames per second (fps). The first frame of the simple reach-to-grasp task was defined as the frame when the affected hand appeared at the rectangle hole. The last frame was defined as the frame when the same hand was back to the rectangle hole while grasping the

apple. The number of the total frames from first to last frame was counted by two experimenters. The time to retrievals was calculated by the multiplication of the number of frames and the inverse fps. When the monkey did not reach their affected hand or could not reach and grasp the apple successfully through the session, we defined the data as empty values and excluded them from the statistical analysis.

Analysis of vertical slit task

The successful trial was defined by grasping the apple with the affected hand and retrieving the apple to the cage without dropping it. The success or failure of the trial was recorded by two experimenters. The success rate for the vertical slit was calculated by the number of successful trials divided total trials per session. The time to retrievals were also calculated. The first frame of the simple reach-to-grasp task was defined as the frame when the affected hand was appeared in the capture. The last frame was defined as the frame when the same hand was backed to the cage while grasping the apple. The number of the total frames from first to last frame was counted by two experimenters. The time to retrievals was calculated describing above.

Calculation of the performance score

The performance score for time to retrievals both in the simple reach-to-grasp task and in the vertical slit task was calculated as follows: *Performance score of the day X = (average time to retrievals of the day X – average time to retrievals of the first assessment day after injection) / (average time to retrievals of the top of the two values during the pre-injection last 5 days – average time to retrievals of the first assessment day after injection).*

Similarly, the performance score for successful retrievals in the vertical slit task was calculated as follows: *Performance score of the day X = (average success rate of the day X – average success rate of the first assessment day after injection) / (average success rate of the top of the two values during the pre-injection last 5 days – average time to retrievals of the first assessment day after injection).*

These calculations yielded 1 as the value of pre-injection and 0 as that of the first assessment day for each monkey; therefore, it became possible to compare the recovery of monkeys with different severities.

Stroke and lesion confirmation

To evaluate the stroke extent, MRI scans were also performed 7 or 14 days and from 3 to 9 months after collagenase injection (Fig. S13A). The imaging protocols consisted of a FLAIR images, repetition time (TR)/echo time (TE), 10,000/101 ms; number of excitations (NEX), 256 × 256; flip

angle, 180°; field of view, 180 mm × 180 mm; matrix, 466 ×512; and slice thickness, 2.6 mm. The unbiased volumes of the stroke were calculated on the basis of Cavalieri's principle (*64*) by using the StereoInvestigator imaging software (MBF Bioscience, Williston, VT). The size and location of the lesion induced by collagenase injection were also evaluated by histological analysis, using the procedure employed in our previous studies (*59, 60*). After the behavioral experiment was completed, brain sections were prepared as in our previous studies (*65-67*). Briefly, the macaques were deeply anesthetized with intravenous injection of sodium pentobarbital (20–30 mg/kg) and then perfused through the ascending aorta with 0.5 L saline containing 2 mL (2,000 units) of heparin sodium followed by fixative containing 10% formaldehyde. The brains were subsequently removed and blocked in the coronal plane (3-mm thick). Brain segments were sectioned coronally at a thickness of 5–6 μm and then stained with Klüver-Barrera staining using standard protocols. Images of the Klüver-Barrera-stained sections were photographed by a BIOREVO BZ-9000 microscope (Keyence) (Fig. S13C).

Pharmacokinetics profiles after single intramuscular administration of edonerpic-maleate in monkeys

The monkeys were fixed with a restraining device at the sampling time points 0.163, 0.333, 0.5, 0.75, 1, 2, 4, or 6 h after intramuscular administration of edonerpic-maleate at doses of 2, 3, or 4 mg/kg. Blood was collected from the lower leg vein at 6 h time point. The obtained plasma samples were stored in a freezer at −80°C, and transported in a frozen state to Toyama Chemical Co., Ltd. The measurement of plasma samples was performed within 2 weeks following the blood collection. Quantification of edonerpic was performed by LC/MS/MS in the equivalent method in mice, but standard curve range of edonerpic was 1 to 1,000 ng/mL in plasma.

Statistics and graphs for non-human primate experiments

For comparing the two independent groups, a Mann-Whitney U test was used (see Statistics and graphs for rodent experiments). For analysis of time-dependent changes of motor function, a two-way ANOVA was used. $p < 0.05$ was considered statistically significant. Statistical analyses were conducted with GraphPad Prism 6. In the graphs, the error bars indicated standard error of the mean.
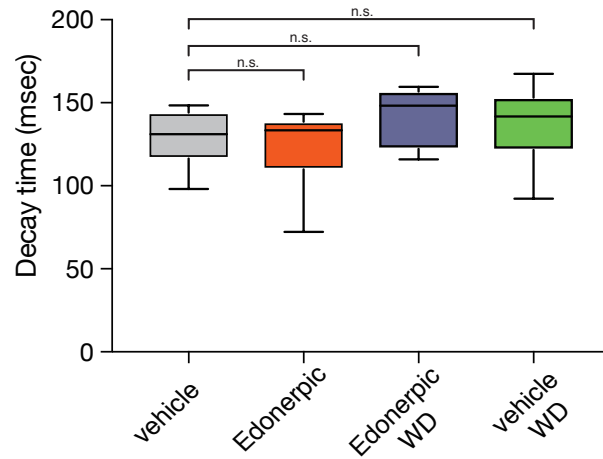
Fig.S1. The effects of edonerpic-maleate on the kinetics of NMDAR-mediated currents.

Average decay time of NMDAR-mediated currents in adult mice treated with vehicle in the presence of intact whisker (Vehicle; n = 10 animals), edonerpic in the presence of intact whisker (Edonerpic; n=10 animals), edonerpic-maleate with whisker deprivation (Edonerpic WD; n = 9 animals) or vehicle with whisker deprivation (Vehicle WD; n = 10 animals). n.s. indicates not significant (one-way ANOVA followed by Dunnett's post hoc test).
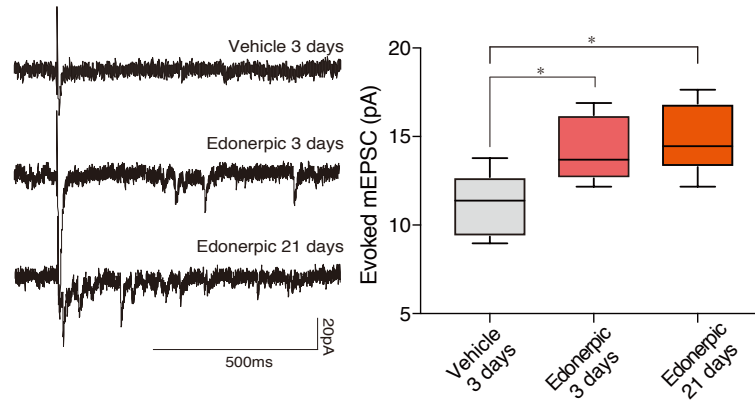
Fig.S2 Three days of application of edonerpic-maleate facilitates synaptic delivery of AMPAR in the barrel cortex

(Left) Evoked quantal EPSC responses at layer 4-2/3 pyramidal synapses in the barrel cortex of adult mice treated with vehicle for 3 days (vehicle, 3 days; n=8 animals), edonerpic-maleate for 3 days (Edonerpic, 3 days; n=8 animals) or edonerpic-maleate for 21 days (Edonerpic, 21 days; n=9 animals). Scale bars, 20pA (vertical), 500ms (horizontal). (Right) Average amplitude of evoked quantal EPSCs. *$p<0.05$ (one-way ANOVA followed by Dunnett's post hoc test).
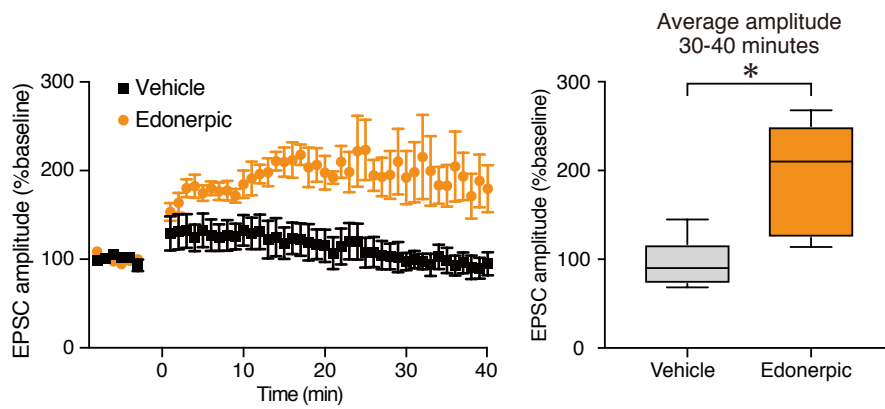
Fig.S3 Edonerpic-maleate facilitates the induction of LTP

(Left) Recordings from cortical slices incubated with edonerpic-maleate (n = 5 animals) or vehicle (n = 6 animals). LTP was induced by a pairing protocol consisting of presynaptic fiber stimulation at 1 Hz for 180 sec paired with postsynaptic depolarization at -40 mV holding potential at layer 4–2/3 pyramidal synapses. The amplitudes of EPSC were normalized to the average baseline amplitude before pairing. (Right) Average EPSC amplitudes in 30–40 min. *$p < 0.05$ (unpaired t-test).
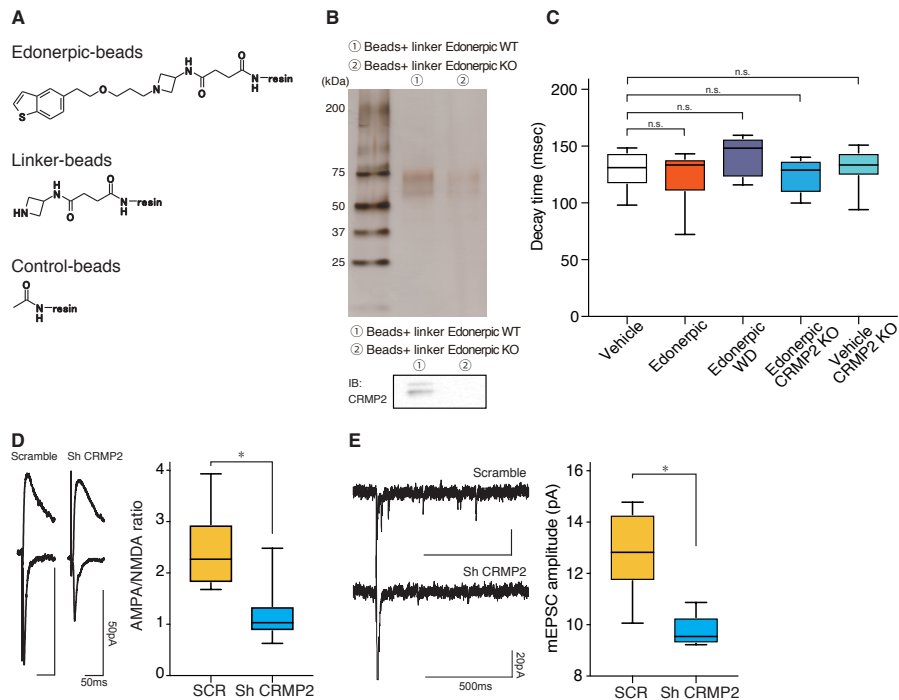
Fig.S4 Characterization of Edonerpic-CRMP2-complex.

(A) The structures of carrier compounds used for affinity purification.

(B) (top) Silver stained gel showing edonerpic-binding proteins from cortical lysate of wild type mice or CRMP2 deficient mice. (bottom) Immunoblot of CRMP2 in cortical lysate from wild type mice or CRMP2 deficient mice pulled down by beads with linker edonerpic.

(C) The data of the wild type animals shown here were derived from Fig.S1. The data of CRMP2 deficient mice treated with edonerpic-maleate (Edonerpic CRMP2 KO; n = 12 animals) and CRMP2 deficient mice treated with Vehicle (Vehicle CRMP2 KO; n = 12 animals) were added. n.s. indicates not significant (one-way ANOVA followed by Dunnett's post hoc test).

(D) (left) Synaptic responses from Sh CRMP2-expressing (Sh CRMP2) or scrambled control-shRNA-expressing (SCR) pyramidal neurons at layer 4-2/3 of wild-type adult barrel cortex of mice administered with edonerpic-maleate. Scale bars: 50 pA, 50 ms. (right) Average A/N ratio. SCR: n=9 animals; Sh CRMP2: n=10 animals. *$p < 0.05$ (Mann-Whitney U test).

(E) (left) Evoked mEPSC from Sh CRMP2-expressing or SCR-expressing neurons at layer 4 - 2/3 pyramidal synapses in the barrel cortex of adult mice administered with edonerpic-maleate. (right) Average amplitude of evoked quantal EPSCs. SCR: n=7 animals; Sh CRMP2: n=7 animals. *$p < 0.05$ (unpaired t-test).
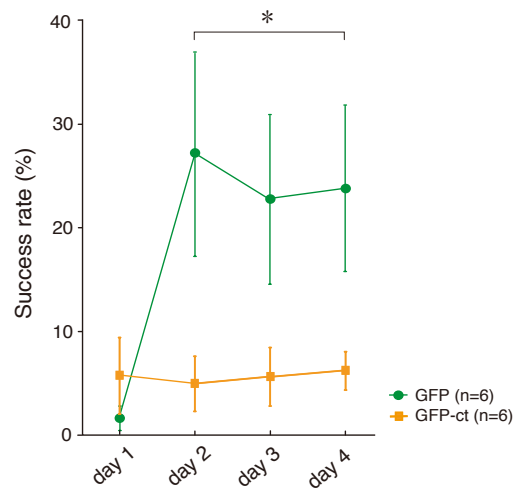
Fig.S5 Expression of GFP-GluA1-ct in the forelimb area in motor cortex prevents the acquisition of reaching task.

 Average success rates in the reaching task in mice injected with GFP-tagged GluA1 c-tail (GFP-GluA1-ct) or GFP expressing lentivirus at the layer 5 in the motor cortex forelimb area. $*p<0.05$, GFP-GluA1-ct vs GFP in day 2, 3 and 4 (two-way ANOVA followed by Bonferroni's post hoc test).
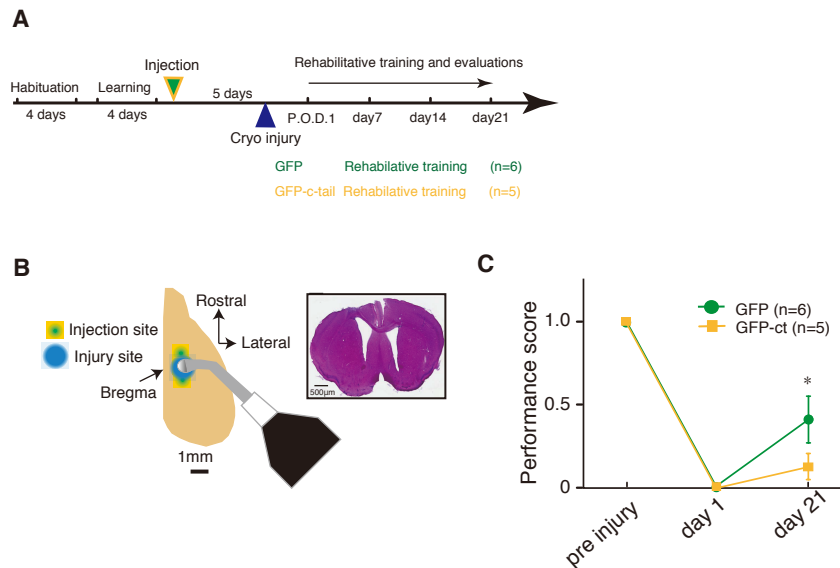
Fig.S6 Synaptic AMPAR delivery-dependent recovery after mild cortical cryoinjury.

(A) Experimental design. (B) (left) Schematic illustration of injection and injury site. (right) Representative of Hematoxylin-Eosin stained coronal sections including the mild cryoinjury. Scale bar, 500 μm.(C) Average performance scores in the reaching task of mice injected with GFP-tagged GluA1 c-tail (GFP-ct) or GFP expressing lentivirus using animals with mild cryoinjury. * $p<0.05$ in day 21 (two-way ANOVA followed by Bonferroni's post hoc test).
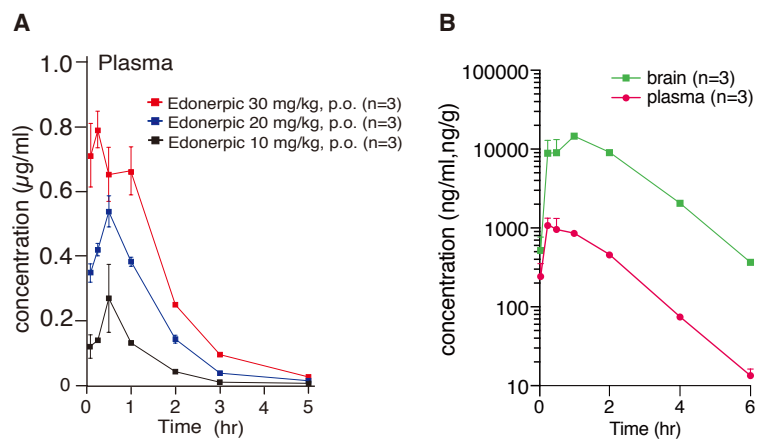
Fig.S7 Concentration-time profiles of edonerpic in mice.

(A) Average plasma concentration after a single oral administration of edonerpic-maleate in mice (10 mg/kg, 20 mg/kg or 30 mg/kg). (B) Brain and plasma levels of edonerpic after a single oral administration of edonerpic-maleate (30 mg/kg) in mice.
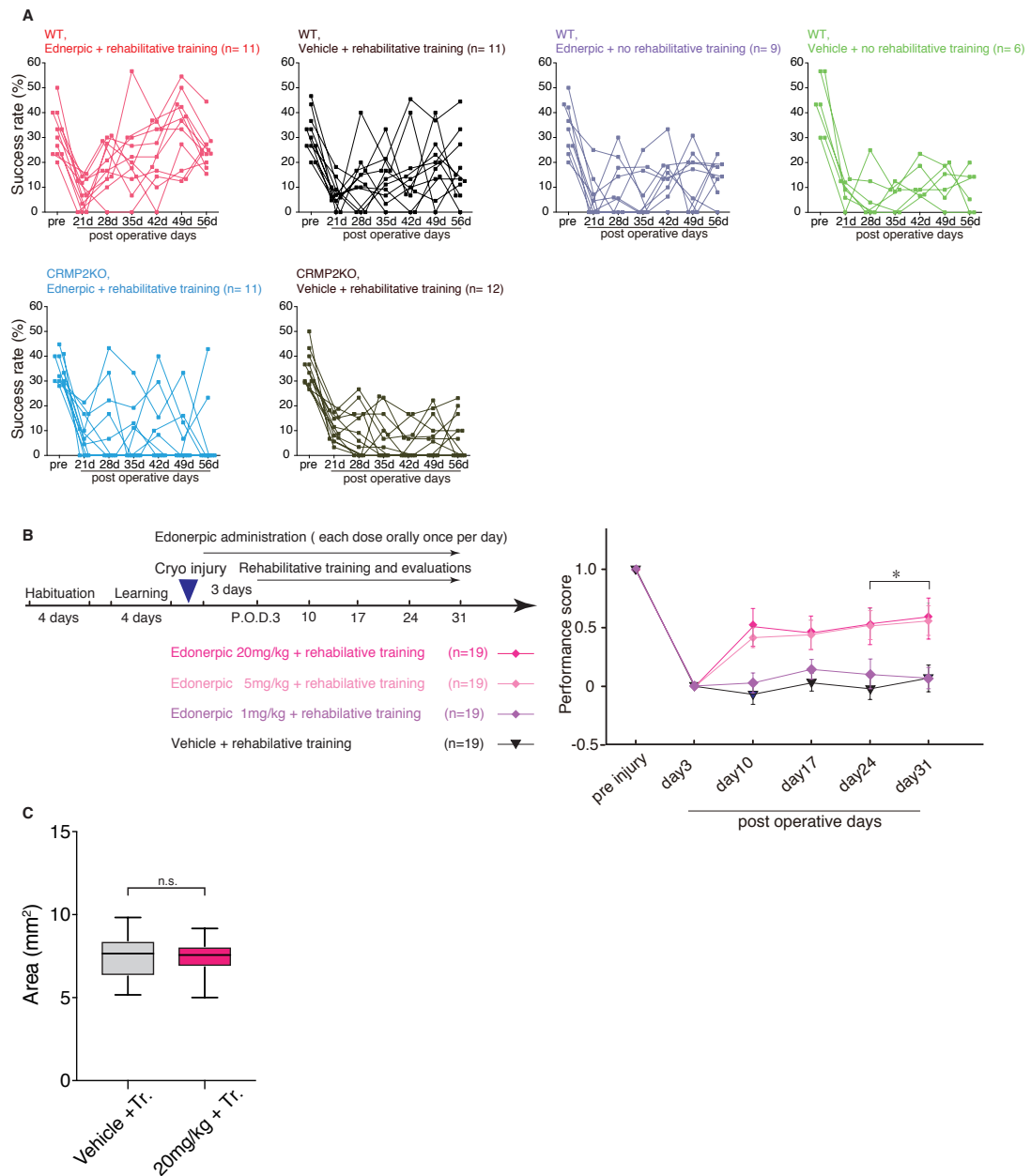
Fig.S8 The individual time course of the success rate and effective doses of edonerpic-maleate on motor function recovery.

(A) The individual time course of the success rate of the reaching task after cryogenic injury in wild type and CRMP2 KO mice. (related to Fig2D). (B)(Left) Experimental design of the treatment with different doses of edonerpic (1, 5, 20 mg/kg, orally, once a day). In this experiment, edonerpic-maleate was administered one day after the cryoinjury. 3 days after the cryoinjury, we started training. Edonerpic-maleate (20 mg/kg) with rehabilitative training (n=19), 5 mg/kg with rehabilitative training (n=19), 1 mg/kg with rehabilitative training (n=19), vehicle with rehabilitative training (n=19). This

experiment was conducted under the double-blinded condition. (Right) Average performance scores of each four groups. Note that two doses of edonerpic-maleate (5 and 20 mg/kg) showed significantly higher performance scores compared to the 1 mg/kg dose or vehicle. *$p<0.05$, 5 or 20 mg/kg vs 1 mg/kg or Vehicle on day 24 and 31 (two-way ANOVA followed by Bonferroni's post hoc test). (C) The injured area of mice treated with Edonerpic-maleate (20 mg/kg) with rehabilitative training (n=19), vehicle with rehabilitative training (n=18). The area of the injury was measured at day 12 or day 13 after cryoinjury. n.s. indicates not significant (unpaired t-test).
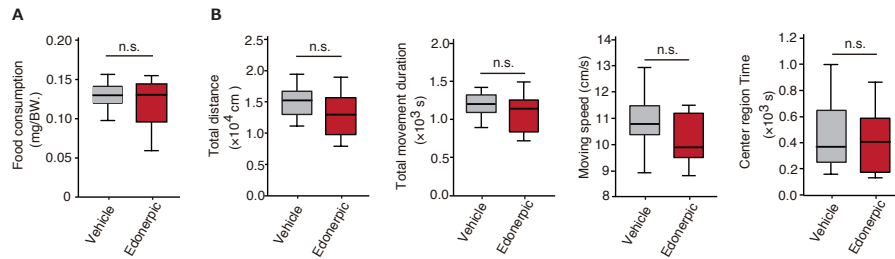
Fig.S9 The effects of edonerpic-maleate on general behaviors.

(A) The amounts of food consumption per body weight. Vehicle n=13, Edonerpic n=13. n.s. indicates not significant (unpaired t-test). (B) Total distance, total movement duration, moving speed and center region time in open field test. Vehicle n=12, Edonerpic n=12**.** n.s. indicates not significant (unpaired t-test).
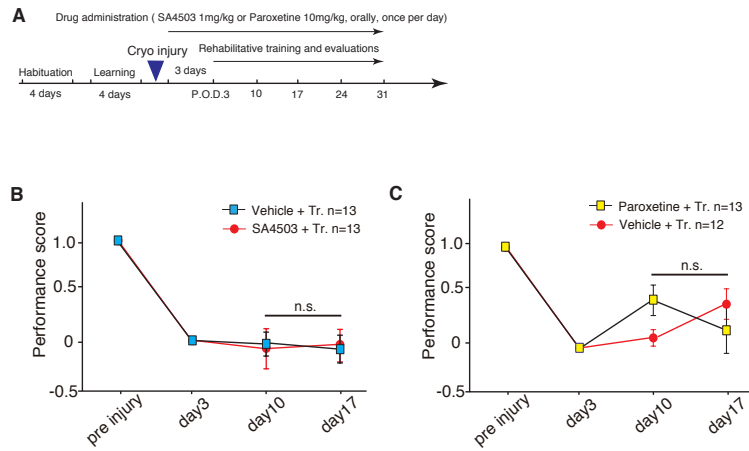
Fig.S10 Application of the selective Sigma1 receptor agonist SA4503 and paroxetine failed to recover motor function after cryoinjury.

(A) Experimental design of treatments with SA4503 (1 mg/kg orally, once a day) or Paroxetine (10 mg/kg orally, once a day). In this experiment, drugs were administered one day after the cryoinjury. 3 days after the cryoinjury, we started training as was in Fig. S8. (B) Average performance scores of cryo-injured mice treated with SA4503. n.s. indicates not significant (two-way ANOVA followed by Bonferroni's post hoc test) (C) Average performance scores of cryo-injured mice treated with Paroxetine. n.s. indicates not significant (two-way ANOVA followed by Bonferroni's post hoc test).
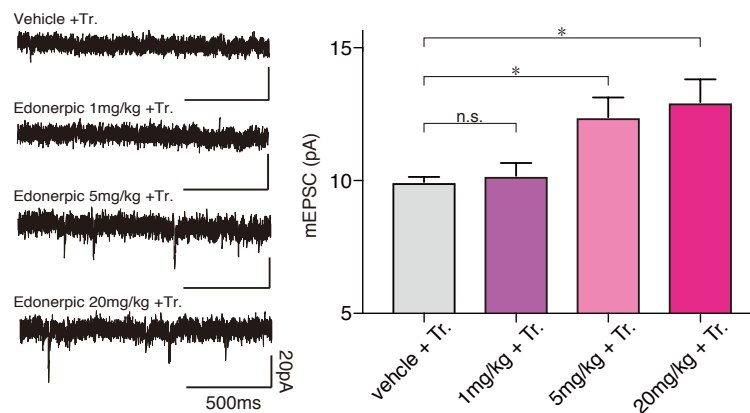
Fig.S11 Effective doses of edonerpic-maleate for the motor functional recovery increase amplitudes of mEPSCs in the peri-injured region of recovered mice.

(Left) Synaptic responses at layer 5 pyramidal neurons in the peri-injured cortical region of mice with different doses of edonerpic-maleate (1, 5, 20 mg/kg, orally, once a day) and rehabilitative training (Tr). Scale bars, 20 pA (vertical), 500 ms (horizontal). (Right) Average amplitudes of mEPSCs. Edonerpic-maleate 20 mg/kg + Tr. (n=3 animals), edonerpic-maleate 5 mg/kg + Tr. (n=4 animals), edonerpic-maleate 1 mg/kg + Tr. (n=4 animals), vehicle + Tr. (n=4 animals). Note that two doses of edonerpic-maleate (5 and 20 mg/kg) showed significantly higher mEPSC amplitude compared to the 1 mg/kg dose or vehicle. *$p<0.05$, 5 or 20 mg/kg + Tr vs 1 mg/kg+ Tr or Vehicle + Tr, n.s. indicates not significant (Kruskal-Wallis test followed by Dunn's post hoc test).
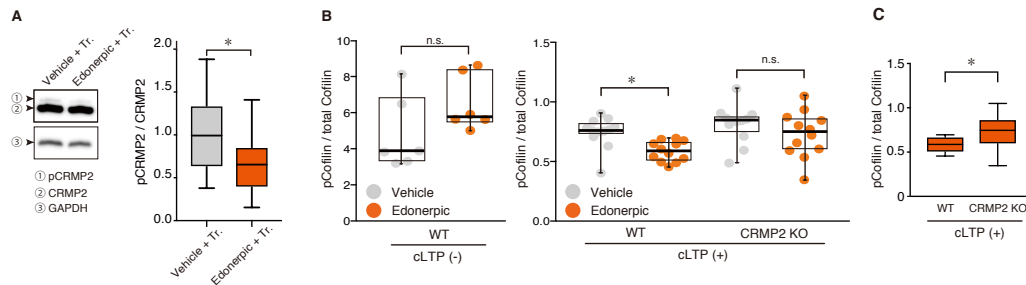
Figure S12 The level of phosphorylated CRMP2 in the peri-injured cortical region and t**he level of phosphorylated ADF/cofilin** in **chemical LTP experiment without data normalization.**

(A) (Left) Immunoblots of CRMP2, phosphorylated CRMP2, and GAPDH in synaptoneurosome fraction obtained from from peri-injured cortical region of mice at day 28 (see Fig. 2D). (Right) Phosphorylation level of CRMP2. The level of CRMP2 and p-CRMP2 were referred to GAPDH. The ratio of p-CRMP2 to CRMP2 was normalized to the vehicle-treated group. Vehicle with rehabilitative training (Vehicle+Tr. n = 13), edonerpic-maleate with rehabilitative training (Edonerpic+Tr. n = 13). *$p < 0.05$ (unpaired t-test).

(B) Phosphorylation level of ADF/cofilin. The level of ADF/cofilin and p-ADF/cofilin were referred to GAPDH. Each point in the graphs indicates the individual data without normalization. cLTP(-) / WT; vehicle n = 6, Edonerpic-maleate n = 6. cLTP(+) / WT; vehicle n = 12, Edonerpic-maleate n = 12. cLTP(+) / KO; vehicle n = 12, Edonerpic-maleate n = 12. n.s. indicates not significant. *$p < 0.05$ (unpaired t-test). (See Fig.3C).

(C) Phosphorylation level of ADF/cofilin in cortical slices of WT or CRMP2 KO mice after cLTP induction applied with edonerpic-maleate. WT: n=12 animals; CRMP2 KO: n=12 animals. *$p < 0.05$ (unpaired t-test).
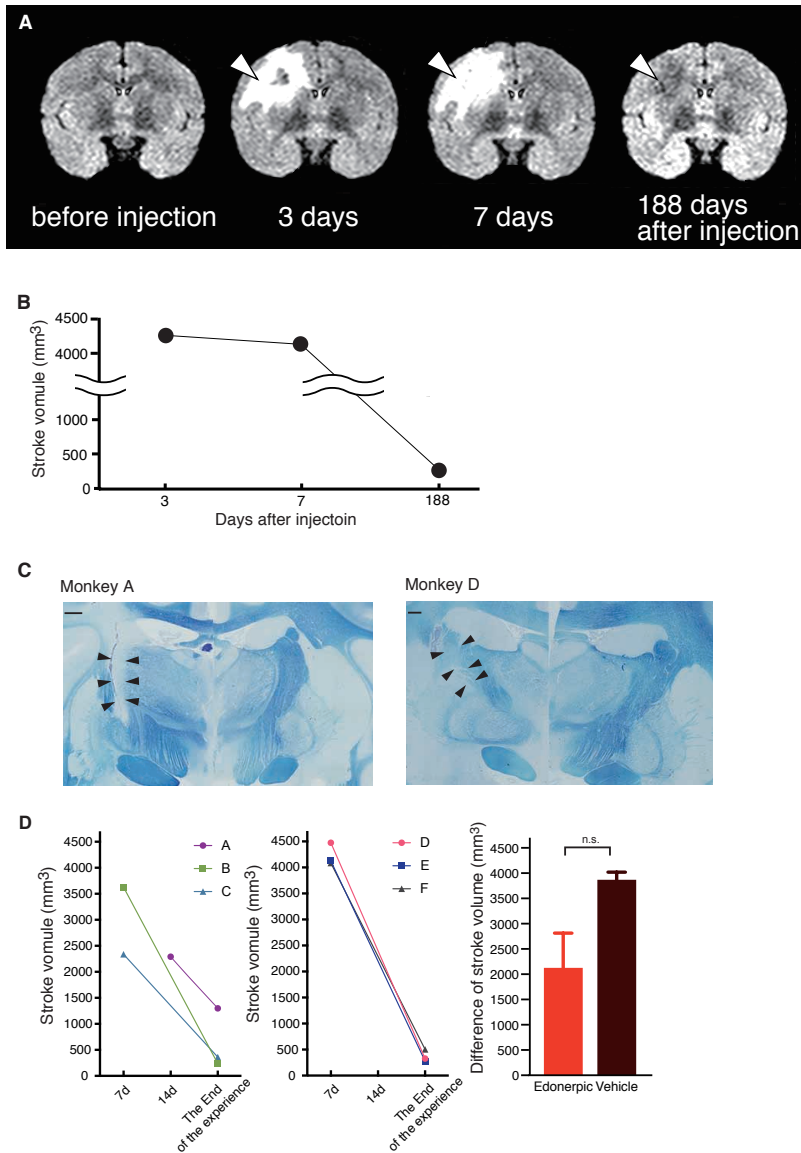
Fig.S13 Sequential MRI scanning and the lesion volume and histological images for the ICH.
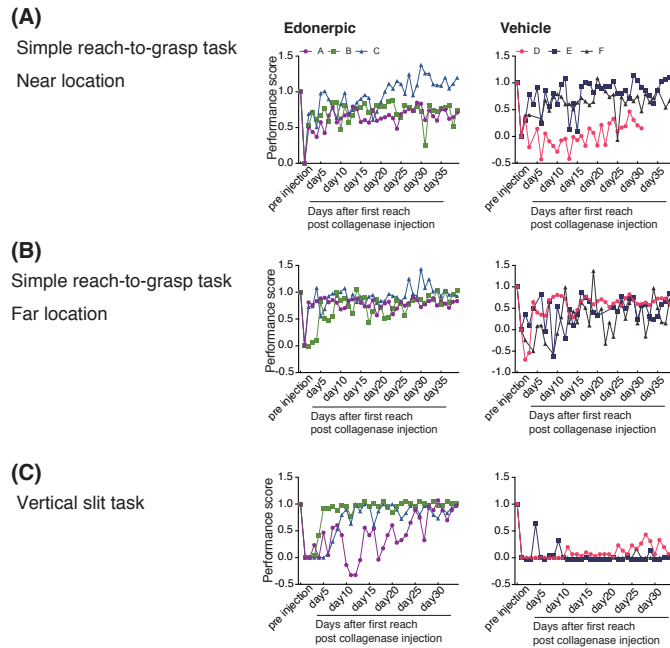
The fluid-attenuated inversion recovery images of MRI scanning before and after collagenase injection (Monkey E). The hyper intense signal area around the injection site which indicated the edema was expanded during 3 days to 7 days after collagenase injection. The edema was diminished 188 days after injection. (B) The stroke volumes (Monkey E) calculated on the basis of Cavalieri's principle. The stroke was large at 3 days and 7 days after collagenase injection, and then reduced in size 188 days after injection. (C) Representative Klüver-Barrera-stained coronal sections including the scars in

the internal capsule (IC). Black arrow heads indicate the scar in the IC. Monkey A treated with edonerpic-maleate, Monkey D treated with vehicle. Scale bars, 1000 μm. (D) (left) The changes of stroke volume in edonerpic-maleate administered monkeys (A, B, C) or vehicle administered monkeys (D, E, F) after collagenase injection. (right) The difference of stroke volumes between 7 days or 14 days after collagenase injection and the end of the experience in edonerpic-maleate administered monkeys (n=3) or vehicle administered monkeys (n=3). n.s. indicates not significant (Mann-Whitney U-test, $p = 0.100$).
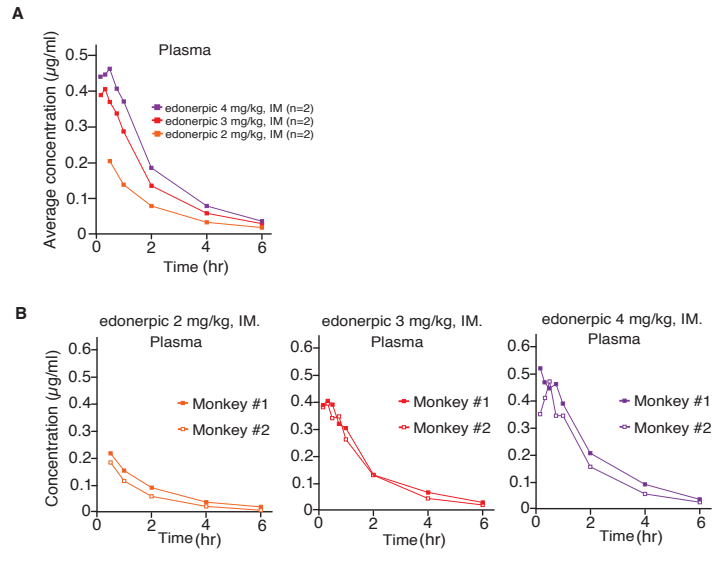
Fig.S14 Concentration-time profiles of edonerpic-maleate in non-human primates.

(A) Average plasma concentration after a single intramuscular administration of edonerpic-maleate 2 mg/kg, 3 mg/kg and 4 mg/kg. (B) Plasma concentration of edonerpic in each animal.

(A)
Simple reach-to-grasp task
Near location

(B)
Simple reach-to-grasp task
Far location

(C)
Vertical slit task

Fig.S15 The individual results of performance scores in simple reach-to-grasp task and vertical slit task. (Monkey A, B, C: edonerpic-maleate- administered monkeys, monkey D, E, F: vehicle-administered monkeys.) (A, B) The individual time course of the performance score for time to retrievals in the simple reach-to-grasp task for the near (A) and the far (B) location. (A) The edonerpic-maleate- administered monkeys showed fast recovery, while the vehicle- administered monkeys, especially monkey D, showed slow recovery. (B) The edonerpic-maleate- administered monkeys showed fast recovery in the early phase and the uniform transition of the performance score, while the vehicle- administered monkeys showed slow recovery and the complex transition of the performance score especially in the early phase. (C) The individual time course of the performance score for successful retrievals in the vertical slit task. The edonerpic-maleate- administered monkey A and B showed fast recovery. Monkey C showed slow recovery, but enough recovery in the late phase of the training period. In contrast, all the vehicle- administered monkeys showed no recovery through the training period.
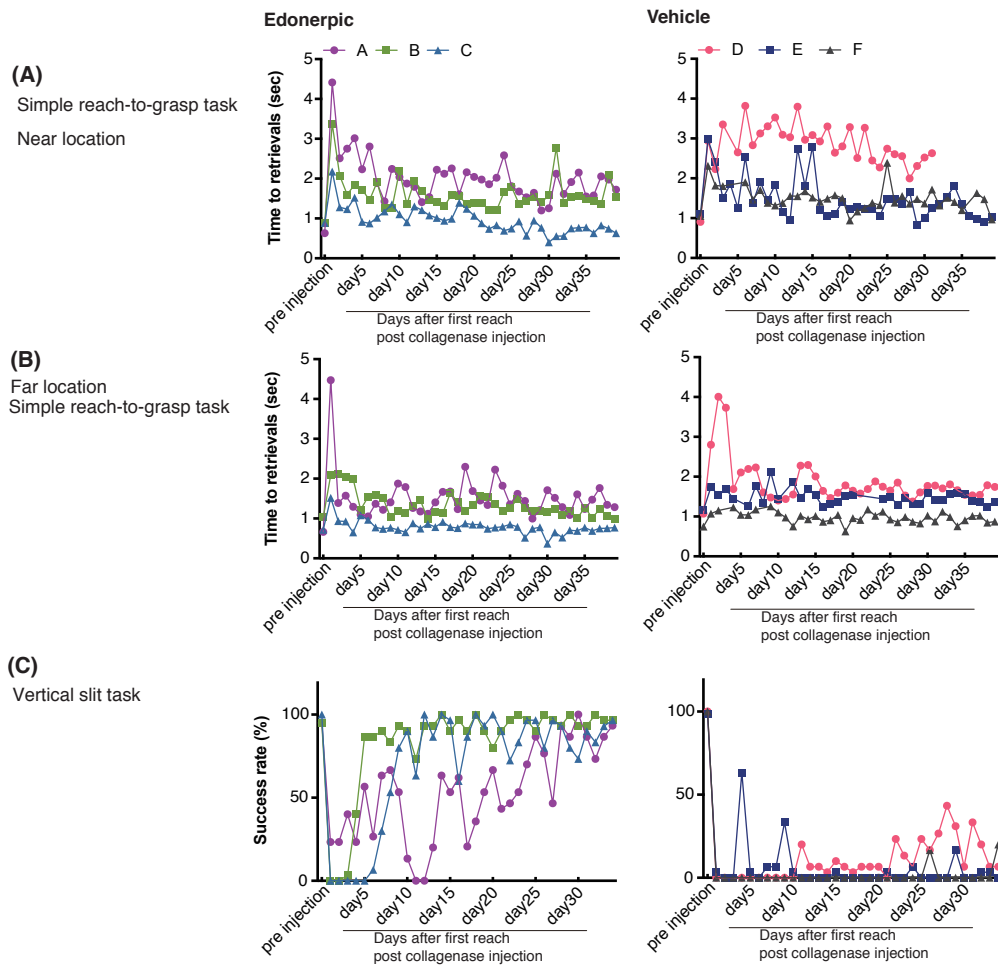
Fig.S16 The individual raw data in non-human primate experience.

(A) The individual raw data of the time to retrievals in simple reach to grasp task for near location.

(B) The individual raw data of the time to retrievals in simple reach to grasp task for far location.

(C) The individual raw data of the success rates in vertical slit task.

Monkey A, B, C: edonerpic-maleate- administered monkeys, monkey D, E, F: vehicle- administered monkeys.

Supplementary movies

Supplementary Movie 1 This movie shows representative movements in simple reach-to-grasp task (near and far location) and vertical slit task before collagenase injection.
Supplementary Movie 2 This movie shows deficits of movements after collagenase injection and changes during the training phase in simple reach-to-grasp task (near location).
Supplementary Movie 3 This movie shows deficits of movements after collagenase injection and changes during the training phase in simple reach-to-grasp task (far location).
Supplementary Movie 4 This movie shows deficits of movements after collagenase injection and changes during the training phase in vertical slit task.

References and Notes

1. T. H. Murphy, D. Corbett, Plasticity during stroke recovery: From synapse to behaviour. *Nat. Rev. Neurosci.* **10**, 861–872 (2009). [doi:10.1038/nrn2735](#) [Medline](#)

2. Y. Murata, N. Higo, T. Hayashi, Y. Nishimura, Y. Sugiyama, T. Oishi, H. Tsukada, T. Isa, H. Onoe, Temporal plasticity involved in recovery from manual dexterity deficit after motor cortex lesion in macaque monkeys. *J. Neurosci.* **35**, 84–95 (2015). [doi:10.1523/JNEUROSCI.1737-14.2015](#) [Medline](#)

3. M. Nishibe, E. T. Urban 3rd, S. Barbay, R. J. Nudo, Rehabilitative training promotes rapid motor recovery but delayed motor map reorganization in a rat cortical ischemic infarct model. *Neurorehabil. Neural Repair* **29**, 472–482 (2015). [doi:10.1177/1545968314543499](#) [Medline](#)

4. M. Nishibe, S. Barbay, D. Guggenmos, R. J. Nudo, Reorganization of motor cortex after controlled cortical impact in rats and implications for functional recovery. *J. Neurotrauma* **27**, 2221–2232 (2010). [doi:10.1089/neu.2010.1456](#) [Medline](#)

5. R. J. Nudo, Mechanisms for recovery of motor function following cortical damage. *Curr. Opin. Neurobiol.* **16**, 638–644 (2006). [doi:10.1016/j.conb.2006.10.004](#) [Medline](#)

6. R. J. Nudo, Neural bases of recovery after brain injury. *J. Commun. Disord.* **44**, 515–520 (2011). [doi:10.1016/j.jcomdis.2011.04.004](#) [Medline](#)

7. R. J. Nudo, B. M. Wise, F. SiFuentes, G. W. Milliken, Neural substrates for the effects of rehabilitative training on motor recovery after ischemic infarct. *Science* **272**, 1791–1794 (1996). [doi:10.1126/science.272.5269.1791](#) [Medline](#)

8. H. W. Kessels, R. Malinow, Synaptic AMPA receptor plasticity and behavior. *Neuron* **61**, 340–350 (2009). [doi:10.1016/j.neuron.2009.01.015](#) [Medline](#)

9. D. Mitsushima, K. Ishihara, A. Sano, H. W. Kessels, T. Takahashi, Contextual learning requires synaptic AMPA receptor delivery in the hippocampus. *Proc. Natl. Acad. Sci. U.S.A.* **108**, 12503–12508 (2011). [doi:10.1073/pnas.1104558108](#) [Medline](#)

10. S. Rumpel, J. LeDoux, A. Zador, R. Malinow, Postsynaptic receptor trafficking underlying a form of associative learning. *Science* **308**, 83–88 (2005). [doi:10.1126/science.1103944](#) [Medline](#)

11. D. Mitsushima, A. Sano, T. Takahashi, A cholinergic trigger drives learning-induced plasticity at hippocampal synapses. *Nat. Commun.* **4**, 2760 (2013). [doi:10.1038/ncomms3760](#) [Medline](#)

12. T. Takahashi, K. Svoboda, R. Malinow, Experience strengthening transmission by driving AMPA receptors into synapses. *Science* **299**, 1585–1588 (2003). [doi:10.1126/science.1079886](#) [Medline](#)

13. J. R. Whitlock, A. J. Heynen, M. G. Shuler, M. F. Bear, Learning induces long-term potentiation in the hippocampus. *Science* **313**, 1093–1097 (2006). [doi:10.1126/science.1128134](#) [Medline](#)

14. R. L. Clem, A. Barth, Pathway-specific trafficking of native AMPARs by in vivo experience. *Neuron* **49**, 663–670 (2006). [doi:10.1016/j.neuron.2006.01.019](#) [Medline](#)

15. S. Jitsuki, K. Takemoto, T. Kawasaki, H. Tada, A. Takahashi, C. Becamel, A. Sano, M. Yuzaki, R. S. Zukin, E. B. Ziff, H. W. Kessels, T. Takahashi, Serotonin mediates cross-modal reorganization of cortical circuits. *Neuron* **69**, 780–792 (2011). doi:10.1016/j.neuron.2011.01.016 Medline

16. T. Miyazaki, K. Takase, W. Nakajima, H. Tada, D. Ohya, A. Sano, T. Goto, H. Hirase, R. Malinow, T. Takahashi, Disrupted cortical function underlies behavior dysfunction due to social isolation. *J. Clin. Invest.* **122**, 2690–2701 (2012). doi:10.1172/JCI63060 Medline

17. H. K. Lee, K. Takamiya, J.-S. Han, H. Man, C.-H. Kim, G. Rumbaugh, S. Yu, L. Ding, C. He, R. S. Petralia, R. J. Wenthold, M. Gallagher, R. L. Huganir, Phosphorylation of the AMPA receptor GluR1 subunit is required for synaptic plasticity and retention of spatial memory. *Cell* **112**, 631–643 (2003). doi:10.1016/S0092-8674(03)00122-3 Medline

18. K. Takemoto, H. Iwanari, H. Tada, K. Suyama, A. Sano, T. Nagai, T. Hamakubo, T. Takahashi, Optical inactivation of synaptic AMPA receptors erases fear memory. *Nat. Biotechnol.* **35**, 38–47 (2017). doi:10.1038/nbt.3710 Medline

19. Y. Goshima, F. Nakamura, P. Strittmatter, S. M. Strittmatter, Collapsin-induced growth cone collapse mediated by an intracellular protein related to UNC-33. *Nature* **376**, 509–514 (1995). doi:10.1038/376509a0 Medline

20. K. Hensley, K. Venkova, A. Christov, W. Gunning, J. Park, Collapsin response mediator protein-2: An emerging pathologic feature and therapeutic target for neurodisease indications. *Mol. Neurobiol.* **43**, 180–191 (2011). doi:10.1007/s12035-011-8166-4 Medline

21. H. Nakamura, N. Yamashita, A. Kimura, Y. Kimura, H. Hirano, H. Makihara, Y. Kawamoto, A. Jitsuki-Takahashi, K. Yonezaki, K. Takase, T. Miyazaki, F. Nakamura, F. Tanaka, Y. Goshima, Comprehensive behavioral study and proteomic analyses of CRMP2-deficient mice. *Genes Cells* **21**, 1059–1079 (2016). doi:10.1111/gtc.12403 Medline

22. K. Kadoyama, K. Matsuura, T. Nakamura-Hirota, M. Takano, M. Otani, S. Matsuyama, Changes in the expression of collapsin response mediator protein-2 during synaptic plasticity in the mouse hippocampus. *J. Neurosci. Res.* **93**, 1684–1692 (2015). doi:10.1002/jnr.23626 Medline

23. K. Hirata, H. Yamaguchi, Y. Takamura, A. Takagi, T. Fukushima, N. Iwakami, A. Saitoh, M. Nakagawa, T. Yamada, A novel neurotrophic agent, T-817MA [1-3-[2-(1-benzothiophen-5-yl) ethoxy] propyl-3-azetidinol maleate], attenuates amyloid-beta-induced neurotoxicity and promotes neurite outgrowth in rat cultured central nervous system neurons. *J. Pharmacol. Exp. Ther.* **314**, 252–259 (2005). doi:10.1124/jpet.105.083543 Medline

24. H. Makihara, S. Nakai, W. Ohkubo, N. Yamashita, F. Nakamura, H. Kiyonari, G. Shioi, A. Jitsuki-Takahashi, H. Nakamura, F. Tanaka, T. Akase, P. Kolattukudy, Y. Goshima, CRMP1 and CRMP2 have synergistic but distinct roles in dendritic development. *Genes Cells* **21**, 994–1005 (2016). doi:10.1111/gtc.12399 Medline

25. J. P. Ip, L. Shi, Y. Chen, Y. Itoh, W.-Y. Fu, A. Betz, W.-H. Yung, Y. Gotoh, A. K. Y. Fu, N. Y. Ip, α2-chimaerin controls neuronal migration and functioning of the cerebral cortex through CRMP-2. *Nat. Neurosci.* **15**, 39–47 (2011). doi:10.1038/nn.2972 Medline

26. K. Ruscher, M. Shamloo, M. Rickhag, I. Ladunga, L. Soriano, L. Gisselsson, H. Toresson, L. Ruslim-Litrus, D. Oksenberg, R. Urfer, B. B. Johansson, K. Nikolich, T. Wieloch, The sigma-1 receptor enhances brain plasticity and functional recovery after experimental stroke. *Brain* **134**, 732–746 (2011). doi:10.1093/brain/awq367 Medline

27. F. Chollet, J. Tardy, J.-F. Albucher, C. Thalamas, E. Berard, C. Lamy, Y. Bejot, S. Deltour, A. Jaillard, P. Niclot, B. Guillon, T. Moulin, P. Marque, J. Pariente, C. Arnaud, I. Loubinoux, Fluoxetine for motor recovery after acute ischaemic stroke (FLAME): A randomised placebo-controlled trial. *Lancet Neurol.* **10**, 123–130 (2011). doi:10.1016/S1474-4422(10)70314-8 Medline

28. J. N. Zhang, U. Michel, C. Lenz, C. C. Friedel, S. Köster, Z. d'Hedouville, L. Tönges, H. Urlaub, M. Bähr, P. Lingor, J. C. Koch, Calpain-mediated cleavage of collapsin response mediator protein-2 drives acute axonal degeneration. *Sci. Rep.* **6**, 37050 (2016). doi:10.1038/srep37050 Medline

29. R. J. Nudo, Recovery after brain injury: Mechanisms and principles. *Front. Hum. Neurosci.* **7**, 887 (2013). doi:10.3389/fnhum.2013.00887 Medline

30. H. Tada, T. Miyazaki, K. Takemoto, K. Takase, S. Jitsuki, W. Nakajima, M. Koide, N. Yamamoto, K. Komiya, K. Suyama, A. Sano, A. Taguchi, T. Takahashi, Neonatal isolation augments social dominance by altering actin dynamics in the medial prefrontal cortex. *Proc. Natl. Acad. Sci. U.S.A.* **113**, E7097–E7105 (2016). doi:10.1073/pnas.1606351113 Medline

31. J. Gu, C. W. Lee, Y. Fan, D. Komlos, X. Tang, C. Sun, K. Yu, H. C. Hartzell, G. Chen, J. R. Bamburg, J. Q. Zheng, ADF/cofilin-mediated actin dynamics regulate AMPA receptor trafficking during synaptic plasticity. *Nat. Neurosci.* **13**, 1208–1215 (2010). doi:10.1038/nn.2634 Medline

32. S. Jitsuki, W. Nakajima, K. Takemoto, A. Sano, H. Tada, A. Takahashi-Jitsuki, T. Takahashi, Nogo receptor signaling restricts adult neural plasticity by limiting synaptic AMPA receptor delivery. *Cereb. Cortex* **26**, 427–439 (2016). doi:10.1093/cercor/bhv232 Medline

33. S. K. Schiemanck, G. Kwakkel, M. W. Post, L. J. Kappelle, A. J. Prevo, Impact of internal capsule lesions on outcome of motor hand function at one year post-stroke. *J. Rehabil. Med.* **40**, 96–101 (2008). doi:10.2340/16501977-0130 Medline

34. C. Rosso, O. Colliot, R. Valabrègue, S. Crozier, D. Dormont, S. Lehéricy, Y. Samson, Tissue at risk in the deep middle cerebral artery territory is critical to stroke outcome. *Neuroradiology* **53**, 763–771 (2011). doi:10.1007/s00234-011-0916-5 Medline

35. R. Wenzelburger, F. Kopper, A. Frenzel, H. Stolze, S. Klebe, A. Brossmann, J. Kuhtz-Buschbeck, M. Gölge, M. Illert, G. Deuschl, Hand coordination following capsular stroke. *Brain* **128**, 64–74 (2005). doi:10.1093/brain/awh317 Medline

36. Y. Murata, N. Higo, Development and characterization of a macaque model of focal internal capsular infarcts. *PLOS ONE* **11**, e0154752 (2016). doi:10.1371/journal.pone.0154752 Medline

37. G. Courtine, M. B. Bunge, J. W. Fawcett, R. G. Grossman, J. H. Kaas, R. Lemon, I. Maier, J. Martin, R. J. Nudo, A. Ramon-Cueto, E. M. Rouiller, L. Schnell, T. Wannier, M. E.

Schwab, V. R. Edgerton, Can experiments in nonhuman primates expedite the translation of treatments for spinal cord injury in humans? *Nat. Med.* **13**, 561–566 (2007). doi:10.1038/nm1595 Medline

38. H. P. Adams Jr., R. J. Nudo, Management of patients with stroke: Is it time to expand treatment options? *Ann. Neurol.* **74**, 4–10 (2013). doi:10.1002/ana.23948 Medline

39. S. Barbay, E. J. Plautz, E. Zoubina, S. B. Frost, S. C. Cramer, R. J. Nudo, Effects of postinfarct myelin-associated glycoprotein antibody treatment on motor recovery and motor map plasticity in squirrel monkeys. *Stroke* **46**, 1620–1625 (2015). doi:10.1161/STROKEAHA.114.008088 Medline

40. R. J. Nudo, G. W. Milliken, W. M. Jenkins, M. M. Merzenich, Use-dependent alterations of movement representations in primary motor cortex of adult squirrel monkeys. *J. Neurosci.* **16**, 785–807 (1996). Medline

41. K. Hensley, A. Christov, S. Kamat, X. C. Zhang, K. W. Jackson, S. Snow, J. Post, Proteomic identification of binding partners for the brain metabolite lanthionine ketimine (LK) and documentation of LK effects on microglia and motoneuron cell cultures. *J. Neurosci.* **30**, 2979–2988 (2010). doi:10.1523/JNEUROSCI.5247-09.2010 Medline

42. Y. Kawano, T. Yoshimura, D. Tsuboi, S. Kawabata, T. Kaneko-Kawano, H. Shirataki, T. Takenawa, K. Kaibuchi, CRMP-2 is involved in kinesin-1-dependent transport of the Sra-1/WAVE1 complex and axon formation. *Mol. Cell. Biol.* **25**, 9920–9935 (2005). doi:10.1128/MCB.25.22.9920-9935.2005 Medline

43. J. M. Brittain, D. B. Duarte, S. M. Wilson, W. Zhu, C. Ballard, P. L. Johnson, N. Liu, W. Xiong, M. S. Ripsch, Y. Wang, J. C. Fehrenbacher, S. D. Fitz, M. Khanna, C.-K. Park, B. S. Schmutzler, B. M. Cheon, M. R. Due, T. Brustovetsky, N. M. Ashpole, A. Hudmon, S. O. Meroueh, C. M. Hingtgen, N. Brustovetsky, R.-R. Ji, J. H. Hurley, X. Jin, A. Shekhar, X.-M. Xu, G. S. Oxford, M. R. Vasko, F. A. White, R. Khanna, Suppression of inflammatory and neuropathic pain by uncoupling CRMP-2 from the presynaptic Ca^{2+} channel complex. *Nat. Med.* **17**, 822–829 (2011). doi:10.1038/nm.2345 Medline

44. D. S. Tukey, E. B. Ziff, Ca2+-permeable AMPA (α-amino-3-hydroxy-5-methyl-4-isoxazolepropionic acid) receptors and dopamine D1 receptors regulate GluA1 trafficking in striatal neurons. *J. Biol. Chem.* **288**, 35297–35306 (2013). doi:10.1074/jbc.M113.516690 Medline

45. M. D. Murphy, D. J. Guggenmos, D. T. Bundy, R. J. Nudo, Current challenges facing the translation of brain computer interfaces from preclinical trials to use in human patients. *Front. Cell. Neurosci.* **9**, 497 (2016). Medline

46. M. Aach, O. Cruciger, M. Sczesny-Kaiser, O. Höffken, R. Ch. Meindl, M. Tegenthoff, P. Schwenkreis, Y. Sankai, T. A. Schildhauer, Voluntary driven exoskeleton as a new tool for rehabilitation in chronic spinal cord injury: A pilot study. *Spine J.* **14**, 2847–2853 (2014). doi:10.1016/j.spinee.2014.03.042 Medline

47. T. Yamashita, W. Liu, Y. Matsumura, R. Miyagi, Y. Zhai, M. Kusaki, N. Hishikawa, Y. Ohta, S. M. Kim, T. H. Kwak, D. W. Han, K. Abe, Novel therapeutic transplantation of induced neural stem cells for stroke. *Cell Transplant.* **26**, 461–467 (2016). Medline

48. T. Xu, X. Yu, A. J. Perlik, W. F. Tobin, J. A. Zweig, K. Tennant, T. Jones, Y. Zuo, Rapid formation and selective stabilization of synapses for enduring motor memories. *Nature* **462**, 915–919 (2009). doi:10.1038/nature08389 Medline

49. M. Tabuse, M. Yaguchi, S. Ohta, T. Kawase, M. Toda, A simple behavioral test for locomotor function after brain injury in mice. *J. Clin. Neurosci.* **17**, 1412–1416 (2010). doi:10.1016/j.jocn.2010.01.056 Medline

50. K. A. Tennant, D. L. Adkins, N. A. Donlan, A. L. Asay, N. Thomas, J. A. Kleim, T. A. Jones, The organization of the forelimb representation of the C57BL/6 mouse motor cortex as defined by intracortical microstimulation and cytoarchitecture. *Cereb. Cortex* **21**, 865–876 (2011). doi:10.1093/cercor/bhq159 Medline

51. R. Paylor, M. Nguyen, J. N. Crawley, J. Patrick, A. Beaudet, A. Orr-Urtreger, Alpha7 nicotinic receptor subunits are not necessary for hippocampal-dependent learning or sensorimotor gating: A behavioral characterization of Acra7-deficient mice. *Learn. Mem.* **5**, 302–316 (1998). Medline

52. S. Shi, Y. Hayashi, J. A. Esteban, R. Malinow, Subunit-specific rules governing AMPA receptor trafficking to synapses in hippocampal pyramidal neurons. *Cell* **105**, 331–343 (2001). doi:10.1016/S0092-8674(01)00321-X Medline

53. J. Rappsilber, M. Mann, Y. Ishihama, Protocol for micro-purification, enrichment, pre-fractionation and storage of peptides for proteomics using StageTips. *Nat. Protoc.* **2**, 1896–1906 (2007). doi:10.1038/nprot.2007.261 Medline

54. N. Yamashita, T. Ohshima, F. Nakamura, P. Kolattukudy, J. Honnorat, K. Mikoshiba, Y. Goshima, Phosphorylation of CRMP2 (collapsin response mediator protein 2) is involved in proper dendritic field organization. *J. Neurosci.* **32**, 1360–1365 (2012). doi:10.1523/JNEUROSCI.5563-11.2012 Medline

55. E. Niisato, J. Nagai, N. Yamashita, F. Nakamura, Y. Goshima, T. Ohshima, Phosphorylation of CRMP2 is involved in proper bifurcation of the apical dendrite of hippocampal CA1 pyramidal neurons. *Dev. Neurobiol.* **73**, 142–151 (2013). doi:10.1002/dneu.22048 Medline

56. W. Nakajima, S. Jitsuki, A. Sano, T. Takahashi, Sustained enhancement of lateral inhibitory circuit maintains cross modal cortical reorganization. *PLOS ONE* **11**, e0149068 (2016). doi:10.1371/journal.pone.0149068 Medline

57. S. G. West, J. F. Finch, P. J. Curran, Structural equation models with nonnormal variables: Problems and remedies, in *Structural Equation Modeling: Concepts, Issues, and Applications*, R. H. Hoyle, Ed. (1995), pp. 56–75.

58. H. Y. Kim, Statistical notes for clinical researchers: Assessing normal distribution (2) using skewness and kurtosis. *Restor. Dent. Endod* **38**, 52–54 (2013). doi:10.5395/rde.2013.38.1.52 Medline

59. Y. Murata, N. Higo, T. Oishi, A. Yamashita, K. Matsuda, M. Hayashi, S. Yamane, Effects of motor training on the recovery of manual dexterity after primary motor cortex lesion in macaque monkeys. *J. Neurophysiol.* **99**, 773–786 (2008). doi:10.1152/jn.01001.2007 Medline

60. Y. Murata, N. Higo, T. Hayashi, Y. Nishimura, Y. Sugiyama, T. Oishi, H. Tsukada, T. Isa, H. Onoe, Temporal plasticity involved in recovery from manual dexterity deficit after motor cortex lesion in macaque monkeys. *J. Neurosci.* **35**, 84–95 (2015). doi:10.1523/JNEUROSCI.1737-14.2015 Medline

61. J. D. Schmahmann, D. N. Pandya, *Fiber Pathways of the Brain*. (Oxford Univ. Press, 2009), pp. 654.

62. R. J. Morecraft, J. L. Herrick, K. S. Stilwell-Morecraft, J. L. Louie, C. M. Schroeder, J. G. Ottenbacher, M. W. Schoolfield, Localization of arm representation in the corona radiata and internal capsule in the non-human primate. *Brain* **125**, 176–198 (2002). doi:10.1093/brain/awf011 Medline

63. Y. Sugiyama, N. Higo, K. Yoshino-Saito, Y. Murata, Y. Nishimura, T. Oishi, T. Isa, Effects of early versus late rehabilitative training on manual dexterity after corticospinal tract lesion in macaque monkeys. *J. Neurophysiol.* **109**, 2853–2865 (2013). doi:10.1152/jn.00814.2012 Medline

64. T. M. Mayhew, A review of recent advances in stereology for quantifying neural structure. *J. Neurocytol.* **21**, 313–328 (1992). doi:10.1007/BF01191700 Medline

65. N. Higo, T. Oishi, A. Yamashita, K. Matsuda, M. Hayashi, Northern blot and in situ hybridization analyses of MARCKS mRNA expression in the cerebral cortex of the macaque monkey. *Cereb. Cortex* **12**, 552–564 (2002). doi:10.1093/cercor/12.5.552 Medline

66. N. Higo, T. Oishi, A. Yamashita, K. Matsuda, M. Hayashi, Cell type- and region-specific expression of neurogranin mRNA in the cerebral cortex of the macaque monkey. *Cereb. Cortex* **14**, 1134–1143 (2004). doi:10.1093/cercor/bhh073 Medline

67. N. Higo, A. Sato, T. Yamamoto, Y. Nishimura, T. Oishi, Y. Murata, H. Onoe, K. Yoshino-Saito, F. Tsuboi, M. Takahashi, T. Isa, T. Kojima, SPP1 is expressed in corticospinal neurons of the macaque sensorimotor cortex. *J. Comp. Neurol.* **518**, 2633–2644 (2010). Medline

<論文目録>
主論文

CRMP2-binding compound, edonerpic maleate, accelerates motor function recovery
from brain damage

Hiroki Abe*, Susumu Jitsuki*, WakiNakajima*, Yumi Murata*,

Aoi Jitsuki-Takahashi, Yuki Katsuno, Hirobumi Tada, Akane Sano, Kumiko Suyama,

Nobuyuki Mochizuki, Takashi Komori, Hitoshi Masuyama, Tomohiro Okuda, Yoshio

Goshima, Noriyuki Higo, Takuya Takahashi

(* equal-contribution)

Science, Vol.360, page 50-57, 2018

副論文

なし

参考論文

なし